Tantalum Borollide Trichloride: A Versatile Entry into Tantalum Borollide Complexes

Caroline K. Sperry, W. Donald Cotter, Rip A. Lee, Rene J. Lachicotte, and Guillermo C. Bazan*,†

Contribution from the Department of Chemistry, University of Rochester, Rochester, New York 14627-0216

Received December 10, 1997

Abstract: The reaction of $Li_2[C_4H_4B\text{-}N(CHMe_2)_2]\cdot THF$ with 2 equiv of $AlCl_3$ and 1 equiv of $TaCl_5$ gives mononuclear $[C_4H_4B\text{-}N(CHMe_2)_2]TaCl_3$ (**1**) in 47% yield. Alkylation of **1** with 3 equiv of MeMgCl gives methylated species in conjunction with the triple decker complex $[C_4H_4B\text{-}N(CHMe_2)_2]Me_2Ta[\mu\text{-}C_4H_4B\text{-}N(CHMe_2)_2]TaMe_4$ (**2**). Monoalkylation is possible with $LiCH(SiMe_3)_2$ to give $[C_4H_4B\text{-}N(CHMe_2)_2]TaCl_2[CH(SiMe_3)_2]$ (**3**) which contains a Ta−C_α−H agostic interaction. Addition of H_2NAr (Ar = 2,6-^{i}Pr$_2$-C_6H_3) and triethylamine to **1** affords $[C_4H_4B\text{-}NH(CHMe_2)_2]Ta(NAr)Cl_2$ (**4**). When 2 equiv of acetone are added to **1**, the result is $[C_4H_4B\text{-}NH(CHMe_2)_2]TaCl_3[Me_2C(O)CH_2C(O)Me]$ (**5**). Reaction with LiCp* (Cp* = C_5Me_5) gives $Cp^*[C_4H_4B\text{-}N(CHMe_2)_2]TaCl_2$ (**6**). Reduction of **6** with Mg under an atmosphere of CO produces $Cp^*[C_4H_4B\text{-}N(CHMe_2)_2]Ta(CO)_2$ (**7**) which can be protonated with $[H(OEt_2)_2][B(C_6H_3(CF_3)_2)_4]$ to form $\{Cp^*[C_4H_4B\text{-}NH(CHMe_2)_2]Ta(CO)_2\}\{[B(C_6H_3(CF_3)_2)_4]\}$ (**8**). Reaction of **1** with excess LiCp′ (Cp′ = C_5H_4Me) affords $Cp'_2[\eta^2\text{-}C_4H_4B\text{-}N(CHMe_2)_2]TaCl$ (**10**) in which the borole ligand is η^2-bound. Addition of $Li[C_5H_5B\text{-}R]$ to **1** results in the formation of $[C_4H_4B\text{-}N(CHMe_2)_2][C_5H_5B\text{-}R]TaCl_2$ (**11**, R = Ph; **12**, R = NMe_2). Methylation of **11** affords $[C_4H_4B\text{-}N(CHMe_2)_2][C_5H_5B\text{-}Ph]TaMe_2$ (**14**), which reacts with H_2 in the presence of PMe_3 to give $[C_4H_4B\text{-}N(CHMe_2)_2][C_5H_5B\text{-}Ph]Ta(PMe_3)_2$ (**16**). For PEt_3, the product is $[C_4H_4B\text{-}N(CHMe_2)_2][C_5H_5B\text{-}Ph]Ta(H)_2PEt_3$ (**17**). Reduction of **1** in the presence of PMe_3 under nitrogen gives $\{[C_4H_4B\text{-}N(CHMe_2)_2](Me_3P)_2ClTaN\}_2$ (**18**). Under an argon atmosphere the reduced product is $[C_4H_4B\text{-}N(CHMe_2)_2]Ta(PMe_3)_3Cl$ (**19**). Complex **19** reacts with hydrogen to give the asymmetric dinuclear complex $([C_4H_4B\text{-}N(CHMe_2)_2]Ta(H)(PMe_3)Cl)\mu\text{-}H([C_4H_4B\text{-}N(CHMe_2)_2]Ta(PMe_3)_2Cl)$ (**20**). The crystallographic characterization of complexes **1**, **3**, **4**, **5**, **7**, **10**, **11**, **12**, **16**, **17**, **18**, **19**, and **20** is also presented. These data give important insight into the metal−borollide relationship under a variety of ligand environments and different oxidation states. They also allow for an estimation of the contribution from the possible resonance forms.

Introduction

Recent work has shown that electrophilic complexes containing boratacyclic ligands can have their reactivity modulated by adjusting the orbital overlap between boron, the exocyclic substituent on boron, and the metal.[1] As is the case for low valent complexes, π donors on boron, such as dialkylamines, weaken the boron−metal interaction.[2] When weak donors, such as methyl or phenyl, are present, the orbital overlap between boron and the metal increases. Since boron is electron deficient, increasing this interaction accentuates the electrophilicity of the metal.

Borollide is a close structural relative of cyclopentadienyl. Its dianionic charge can be understood in terms of an isoelectronic replacement of C with B^-. The group 4 complexes $Cp^*[C_4H_4B\text{-}N(CHMe_2)_2]M(\mu\text{-}Cl_2)Li(OEt_2)_2$ (Cp* = C_5Me_5, M = Zr, Hf) are amphoteric and can participate in heterolytic bond-activation reactions.[3] The tantalum complex $Cp^*[C_4H_4B\text{-}N(CHMe_2)_2]TaMe_2$ is isostructural with standard group 4 metallocenes and displays similar reactivity, including polymerization of ethylene.[4]

Aminoborollide-metal bonding may include contributions from three limiting resonance structures: **A** [M(d^n)-(dianionic borollide)], **B** [M(d^{n+2})-(diolefin π complex)], and **C** [M(d^n)-(metallacyclopentene)].[5] Herberich's work shows that form **B** best describes the structures of low valent complexes.[2a] Bercaw and co-workers have noted that each structure can be classified according to Green's CBC formalism[6] as **A** ($\eta^5\text{-}L_2Z = \eta^5\text{-}LX_2$), **B** ($\eta^4\text{-}L_2$), and **C** ($\eta^4\text{-}LX_2$). For tantalum−borollide complexes, elongated metal−boron distances and a strong interaction between boron and sp^2 hybridized nitrogen are observed, indicating that resonance structures **B** and **C** are major contributors.

Protonated aminoborollides and methylborollide complexes, such as $\{Cp^*[C_4H_4B\text{-}NH(CHMe_2)_2]TaMe_2\}\{B(C_6F_5)_4\}$ and $Cp^*[C_4H_4BMe]TaMe_2$, contain shorter tantalum−boron bond distances than those of aminoborollide analogues.[4,7] When the

† Current address: Department of Chemistry, University of California, Santa Barbara, CA 93106.

(1) For a recent review, see: Herberich, G. E. In *Comprehensive Organometallic Chemistry II*; Abel, E. W., Stone, F. G. A., Wilkinson, G., Eds.; Pergamon Press: Oxford, 1995; Vol. 1, p 197. For vanadium complexes, see: Herberich, G. E.; Hausmann, I.; Klaff, N. *Angew. Chem., Int. Ed. Engl.* **1989**, *23*, 319.

(2) (a) Herberich, G. E.; Hessner, B.; Ohst, H.; Raap, I. A. *J. Organomet. Chem.* **1988**, *348*, 305 (b) Herberich, G. E.; Hostalek, M.; Laven, R.; Boese, R. *Angew. Chem., Int. Ed. Engl.* **1990**, *29*, 317.

(3) Quan, R. W.; Bazan, G. C.; Kiely, A. F.; Schaefer, W. P.; Bercaw, J. E. *J. Am. Chem. Soc.* **1994**, *116*, 4489.

(4) Bazan, G. C.; Donnelly, S. J.; Rodriguez, G. *J. Am. Chem. Soc.* **1995**, *117*, 2671.

(5) (a) Pastor, A.; Kiely, A. F.; Henling, L. M.; Day, M. W.; Bercaw, J. E. *J. Organomet. Chem.* **1997**, *528*, 65. (b) Erker, G.; Engel, K.; Krüger, C.; Müller, G. *Organometallics* **1984**, *3*, 128.

(6) Green, M. L. H. *J. Organomet. Chem.* **1995**, *500*, 127.

(7) For the effect on low valent complexes, see: Herberich, G. E.; Negele M.; Ohst, H. *Chem. Ber.* **1991**, *124*, 25.

S0002-7863(97)04188-7 CCC: $15.00
Published on Web 07/23/1998

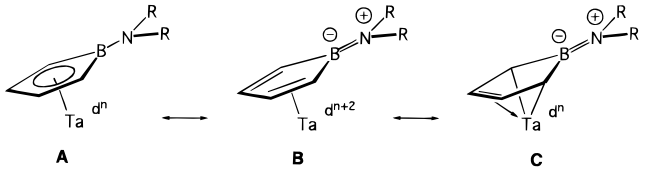

exocyclic substituent cannot participate in π-donation to boron, the contribution from **B** and **C** is significantly reduced. Recent mechanistic work has shown that the rates of elementary chemical reactions and the propensity of the metal to bind substrates are greatly altered by the nature of the exocyclic group.[8] These tantalum complexes are therefore useful for probing mechanistic pathways that may be operative in conventional group 4 metallocenes.

Structural characterization of high valent aminoboratabenzene derivatives, such as $[C_5H_5B\text{-}N(CHMe_2)_2]_2ZrCl_2$, also reveals strong B−N π orbital overlap.[9] The aminoboratabenzene ligand thus binds in a manner similar to the pentadienyl fragment and resonance contribution **D** dominates.

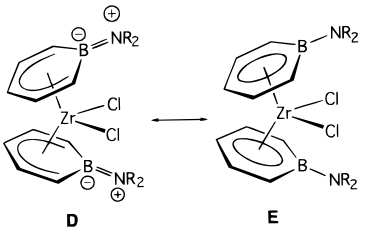

In the case of $[C_5H_5B\text{-}Ph]_2ZrCl_2$ and $[C_5H_5B\text{-}Me]_2ZrCl_2$, only resonance structure **E** can contribute, and the boron−zirconium distance is correspondingly shorter.[10] Differences in metal−boron orbital overlap translate into different catalytic reactivity. For example, while mixing $[C_5H_5B\text{-}N(CHMe_2)_2]_2ZrCl_2$ with MAO (MAO = methylaluminoxane) results in ethylene polymerization catalysis, the reaction of $[C_5H_5B\text{-}OEt]_2ZrCl_2$ with MAO and ethylene gives 1-alkenes exclusively.[11]

The ability to control the metal's reactivity via the boron substituent suggests that boron heterocycles may expand the specificity of homogeneous electrophilic catalysts. These are important considerations in view of their utility in diverse areas of chemistry including C−H activation,[12] hydroaddition reactions (e.g., hydrosilylation[13] and hydroamination[14]), development of reactions for organic transformations,[15] acetylene oligomerization,[16] defluorination of saturated perfluorocarbons,[17] and the polymerization of olefins,[18] silanes,[19] stannanes,[20] and primary phosphines.[21] Recent advances in boron heterocycle synthesis have improved their availability.[22] Increased accessibility of these ligands and their complexes makes widespread application of their chemistry feasible.

Despite this progress, the broad reactivity profile of electrophilic complexes containing boron heterocycles remains largely uncharted compared to the more extensively studied metallocenes. Information about reduced, mono-ring and mixed ring species is noticeably absent. Also lacking is a general understanding of the impact of the amphoteric nature of borollide complexes upon their chemistry. Versatile synthetic intermediates are required if these goals are to be achieved. We report here the preparation and reaction chemistry of one such reagent, $[C_4H_4B\text{-}N(CHMe_2)_2]TaCl_3$.

Results and Discussion

Synthesis of $[C_4H_4B\text{-}N(CHMe_2)_2]TaCl_3$ via Borollide Aluminates. Treatment of tantalum halides with $Li_2[C_4H_4B\text{-}N(CHMe_2)_2]\cdot THF$ frequently presents synthetic difficulties. It is possible to prepare $[C_4H_4B\text{-}N(CHMe_2)_2]TaMe_3(PMe_3)$ from $TaMe_3Cl_2$, $Li_2[C_4H_4B\text{-}N(CHMe_2)_2]\cdot THF$ and PMe_3, but this molecule shows no further substitution chemistry.[23] Direct reaction of $TaCl_5$ with $Li_2[C_4H_4B\text{-}N(CHMe_2)_2]\cdot THF$ results in reduction of the metal, accompanied by the quantitative formation of the Diels−Alder dimer of 1-(diisopropylamino)borole.[24] The metal-containing products are intractable. Formation of the borolene disilicon reagent, by reaction of 2.2 equiv of Me_3SiCl with $Li_2[C_4H_4B\text{-}N(CHMe_2)_2]\cdot THF$,[25] can be accomplished cleanly, but no transmetalation to tantalum was observed when this reagent was treated with either $TaCl_5$, $Ta(OMe)_5$, or TaF_5 under a variety of experimental conditions.[26]

We have found that borollide aluminate complexes, which can be formed in situ, are suitable reagents for transferring borollide to tantalum. Addition of $Li_2[C_4H_4B\text{-}N(CHMe_2)_2]\cdot THF$ to a benzene slurry containing 2 equiv of $AlCl_3$ results in

(8) Kowal, C. M.; Bazan, G. C. *J. Am. Chem. Soc.* **1996**, *118*, 10317.

(9) (a) Bazan, G. C.; Rodriguez, G.; Ashe, A. J., III.; Al-Ahmad, S.; Müller, C. *J. Am. Chem. Soc.* **1996**, *118*, 2291. (b) Ashe, A. J., III.; Kampf, J. W.; Müller, C.; Schneider, M. *Organometallics* **1996**, *15*, 387. (c) Ashe, A. J., III.; Kampf, J. W.; Waas, J. R. *Organometallics* **1997**, *16*, 163.

(10) Bazan, G. C.; Rodriguez, G.; Ashe, A. J., III.; Al-Ahmad, S.; Kampf, J. W. *Organometallics* **1997**, *16*, 2492.

(11) Rogers, J. S.; Bazan, G. C.; Sperry, C. K. *J. Am. Chem. Soc.* **1997**, *119*, 9305.

(12) (a) Walsh, P. J.; Hollander, F. J.; Bergman, R. G. *Organometallics* **1993**, *12*, 3705. (b) Walsh, P. J.; Carney, M. J.; Bergman, R. G. *J. Am. Chem. Soc.* **1991**, *113*, 6343. (c) Walsh, P. J.; Hollander, F. J.; Bergman, R. G. *J. Organomet. Chem.* **1992**, *428*, 13.

(13) (a) Takahashi, T.; Hasegawa, M.; Suzuki, N.; Saburi, M.; Rousset, C. J.; Fanwick, P. E.; Negishi, E. *J. Am. Chem. Soc.* **1991**, *113*, 8564. (b) Kesti, M. R.; Waymouth, R. M. *Organometallics* **1992**, *11*, 1095.

(14) (a) Gagné, M. R.; Stern, C. L.; Marks, T. J. *J. Am. Chem. Soc.* **1992**, *114*, 275. (b) Li, Y.; Fu, P.-F.; Marks, T. J. *Organometallics* **1994**, *13*, 439.

(15) See, for example: (a) Negishi, E.-I. In *Comprehensive Organic Synthesis*; Trost, B. M., Fleming, I., Eds.; Pergamon: Oxford, 1991; Vol. 5, Chapter 9.5, p 1163. (b) Berk, S. C.; Grossman, R. B.; Buchwald, S. L. *J. Am. Chem. Soc.* **1994**, *116*, 8593. (c) Knight, K. S.; Wang, D.; Waymouth, R. M.; Ziller, J. *J. Am. Chem. Soc.* **1994**, *116*, 1845. (d) Jensen, M.; Livinghouse, T. *J. Am. Chem. Soc.* **1989**, *111*, 4495.

(16) (a) Duchateau, R.; Van Wee, C. T.; Meetsma, A.; Teuben, J. H. *J. Am. Chem. Soc.* **1993**, *115*, 4931. (b) Heeres, H. J.; Teuben, J. H. *Organometallics* **1991**, *10*, 1980. (c) Heeres, H. J.; Heeres, A.; Teuben, J. H. *Organometallics* **1990**, *9*, 1508.

(17) Kiplinger, J. L.; Richmond, T. G. *J. Am. Chem. Soc.* **1996**, *118*, 1805.

(18) For recent reviews, see: (a) Brintzinger, H. H.; Fischer, D.; Mülhaupt, R.; Rieger, B.; Waymouth, R. M. *Angew. Chem., Int. Ed. Engl.* **1995**, *34*, 1143. (b) *Ziegler Catalysts*; Fink, G., Mülhaupt, R., Brintzinger, H. H., Eds.; Springer-Verlag: Berlin, 1995. (c) Thayer, A. M. *Chem. Eng. News* **1995**, *73(37)*, 15. (d) Schaverien, C. J. *Adv. Organomet. Chem.* **1994**, *36*, 283. (d) Jordan, R. F. *Adv. Organomet. Chem.* **1991**, *32*, 325. (e) Marks, T. J. *Acc. Chem. Res.* **1992**, *25*, 57.

(19) (a) Harrod, J. F.; Mu, Y.; Samuel, E. *Polyhedron* **1991**, *10*, 1239. (b) Tilley, T. D. *Acc. Chem. Res.* **1993**, *26*, 22, and references therein.

(20) Imori, T.; Lu, B.; Cai, H.; Tilley, T. D. *J. Am. Chem. Soc.* **1995**, *117*, 9931.

(21) Fermin, M. C.; Stephan, D. W. *J. Am. Chem. Soc.* **1995**, *117*, 12645.

(22) (a) Hoic, D. A.; Wolf, J. R.; Davis, W. M.; Fu, G. C. *Organometallics* **1996**, *15*, 1315. (b) Herberich, G. E.; Hessner, B.; Negele, M.; Howard, J. A. K. *J. Organomet. Chem.* **1987**, *336*, 29.

(23) The $[C_4H_4B\text{-}N(CHMe_2)_2]TaMe_3$ complex was observed by NMR spectroscopy, but isolation proved to be impossible. ^{1}H NMR (C_6D_6): δ 5.42 (m, 2H, C*H*CHB), 3.44 (m, 2H, CHC*H*B), 3.46 (sept., 2H, C*H*Me$_2$), 1.11 (d, 12H, CH*Me$_2$*), 0.77 (s, 9H, Ta*Me$_3$*). ^{11}B NMR (external reference $BF_3\cdot OEt_2$): δ 35.8. ^{13}C{^{1}H} NMR (C_6D_6): δ 125.2 (*C*HCHB), 89.8 (CHC*H*B), 47.8 (*C*HMe$_2$), 24.2 (CH*Me$_2$*), 22.9 (Ta*Me$_3$*).

(24) Herberich, G. E.; Ohst, H. *Chem. Ber.* **1985**, *118*, 4303.

(25) Herberich, G. E.; Ohst, H. *Z. Naturforsch.* **1983**, *386*, 1388.

(26) For an example of a trimethylsilylcyclopentadiene reaction with tantalum halides, see: Cardoso, A. M.; Clark, R. J. H.; Moorhouse, S. *J. Chem. Soc., Dalton Trans.* **1980**, 1156.

Scheme 1[a]

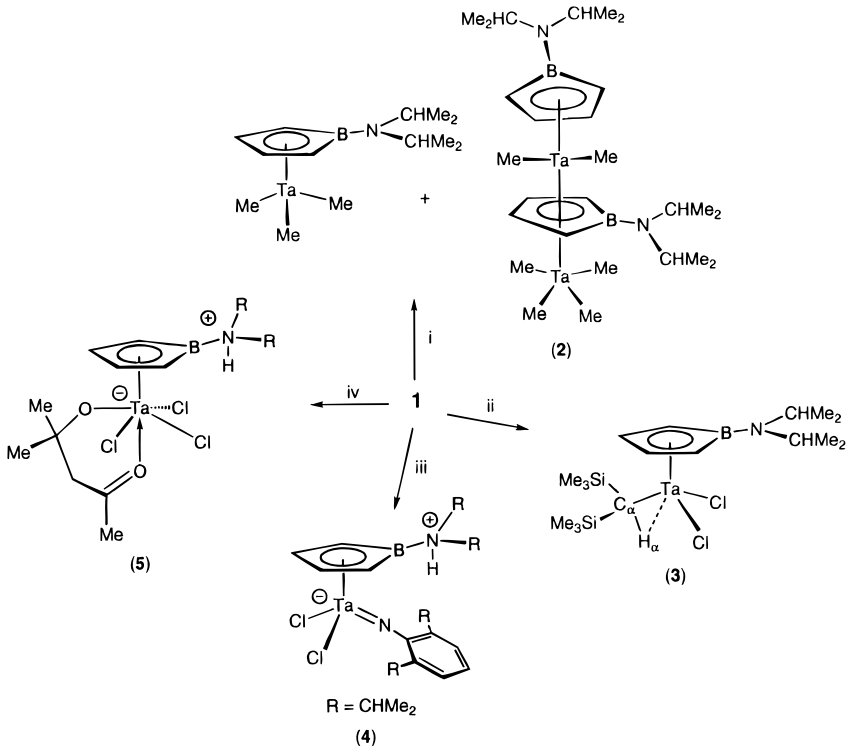

[a] (i) 3.0 equiv of MeMgCl, Et_2O, −35 °C; (ii) 1.0 equiv of $LiCH(SiMe_3)_2$, C_6H_6, room temperature; (iii) 1.0 equiv of $H_2N(2,6\text{-}(CHMe_2)_2C_6H_3)$, 2.0 equiv of NEt_3, C_6H_6, room temperature; (iv) 2.0 equiv of Me_2CO, C_6H_6, room temperature.

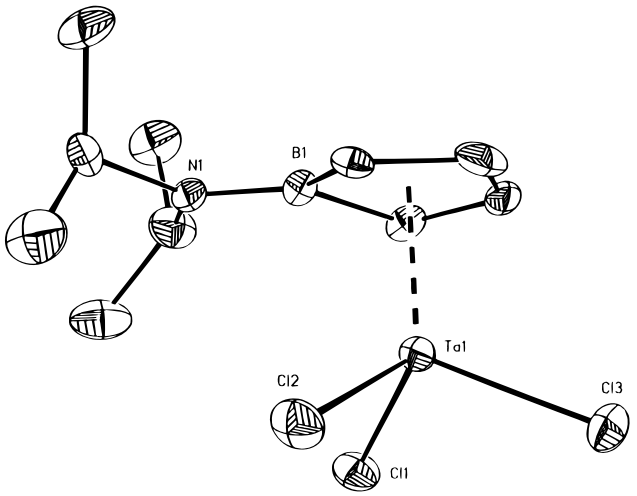

Figure 1. ORTEP drawing of **1** shown at 30% probability. Hydrogen atoms are not shown.

a heterogeneous mixture. Upon addition to a suspension of $TaCl_5$ in benzene, an immediate color change occurs from pale yellow to intense purple. Pentane extraction and crystallization from pentane affords $[C_4H_4B\text{-}N(CHMe_2)_2]TaCl_3$ (**1**) in 47% yield as a deep purple solid (eq 1). Structural characterization of **1** (Figure 1) reveals that the borollide ligand has the typical long Ta−B distance and strong B−N interaction (Table 1). Compound **1** is monomeric in the solid state, in distinct contrast to isoelectronic cyclopentadienylzirconium trichlorides. $CpZrCl_3$ ($Cp = C_5H_5$) has a coordination geometry of infinite chains with bridging chlorides,[27] while Cp^*ZrCl_3 is oligomeric.[28] The monomeric structure of **1** may be a consequence of the ambivalent nature of the borollide ligand. The increased electron density at tantalum in resonance structure **B**, formally Ta(III), renders the metal center less prone to rely on bridging chloride ligands to satisfy its electronic requirements.

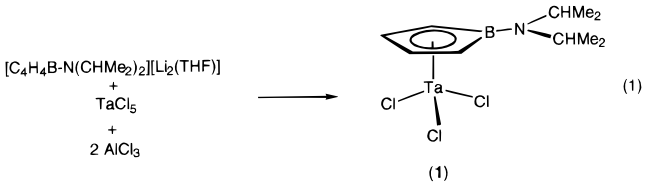

The exact role of $AlCl_3$ as a borollide transfer agent remains unclear since the reaction in benzene is heterogeneous. ^1H NMR spectroscopy reveals that solutions of $AlCl_3$ and $Li_2[C_4H_4B\text{-}N(CHMe_2)_2]$ in THF-d_8 contain several species undergoing dynamic exchange. Removal of solvent results in tacky or gummy solids which could not be characterized. The low solubility of the aluminate intermediates in benzene leads us to believe that they are oligomeric. Despite these mechanistic uncertainties, the reaction in eq 1 is highly reliable and is the only current synthetic entry into **1**.

Substitution Chemistry and Heterolytic Activation Reactions of 1. Alkylations. Treatment of **1** with 3 equiv of MeMgCl or MeLi produces mixtures of alkylated species according to ^1H NMR analysis. A major product in these reactions is the previously reported bimetallic dimer $[C_4H_4B\text{-}N(CHMe_2)_2]Me_2Ta[\mu\text{-}C_4H_4B\text{-}N(CHMe_2)_2]TaMe_4$ (**2**, see Scheme 1).[23] Formation of **2** is minimized at lower temperatures but the selectivity of the reactions remains poor, and the oily nature of the products prevents isolation of mononuclear products.

The reaction of **1** with $LiCH(SiMe_3)_2$ gives $[C_4H_4B\text{-}N(CHMe_2)_2]TaCl_2[CH(SiMe_3)_2]$ (**3** in Scheme 1) as a forest-green microcrystalline solid. Although the reaction is quantitative by ^1H NMR spectroscopy, isolated yields are approximately 60% because of the high solubility of **3** in most common organic

(27) Engelhardt, L. M.; Papasergio, R. I.; Raston, C. L.; White, A. H. *Organometallics* **1984**, *3*, 18.
(28) Poli, R. *Chem. Rev.* **1991**, *91*, 509.

Table 1. Selected Intraligand and Metal−Borollide Distances[a]

	B−N	$C_\alpha-C_\beta$	$C_\beta-C_{\beta'}$	$C_{\beta'}-C_{\alpha'}$	Ta−B	Ta−C_α	Ta−C_β	Ta−$C_{\beta'}$	Ta−$C_{\alpha'}$
1	1.404(14)	1.383(12)	1.401(12)	1.431(12)	2.531(11)	2.308(9)	2.288(9)	2.325(10)	2.322(10)
3	1.412(13)	1.410(14)	1.378(12)	1.433(14)	2.578(10)	2.358(10)	2.333(10)	2.297(9)	2.282(10)
4	1.556(12)	1.414(14)	1.343(12)	1.409(12)	2.544(10)	2.359(9)	2.290(10)	2.369(11)	2.485(9)
5	1.554(6)	1.409(6)	1.339(7)	1.404(6)	2.608(5)	2.433(4)	2.337(4)	2.391(4)	2.520(4)
7	1.448(12)	1.431(12)	1.383(12)	1.397(12)	2.709(13)	2.389(11)	2.245(11)	2.301(12)	2.438(11)
10	1.407(4)	1.464(6)	1.483(6)	1.347(6)		2.270(4)	2.335(4)		
11	1.413(8)	1.447(9)	1.376(9)	1.417(9)	2.717(7)	2.330(6)	2.297(6)	2.379(7)	2.424(6)
12	1.401(12)	1.389(12)	1.437(12)	1.426(12)	2.710(12)	2.408(12)	2.383(12)	2.319(12)	2.336(13)
16	1.442(11)	1.445(10)	1.428(10)	1.416(10)	2.722(8)	2.383(7)	2.273(7)	2.340(7)	2.472(7)
17	1.427(5)	1.430(5)	1.412(5)	1.419(5)	2.699(4)	2.390(4)	2.321(4)	2.334(4)	2.405(4)
18	1.437(10)	1.401(11)	1.415(12)	1.427(11)	2.716(9)	2.486(7)	2.373(8)	2.288(8)	2.359(8)
19	1.420(8)	1.434(8)	1.429(8)	1.421(8)	2.640(6)	2.349(5)	2.243(5)	2.274(5)	2.389(5)
20	1.424(9)	1.457(9)	1.407(9)	1.452(9)	2.718(7)	2.423(6)	2.340(6)	2.300(6)	2.369(6)

[a] Atom designation follows the following scheme:

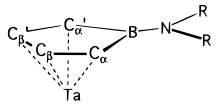

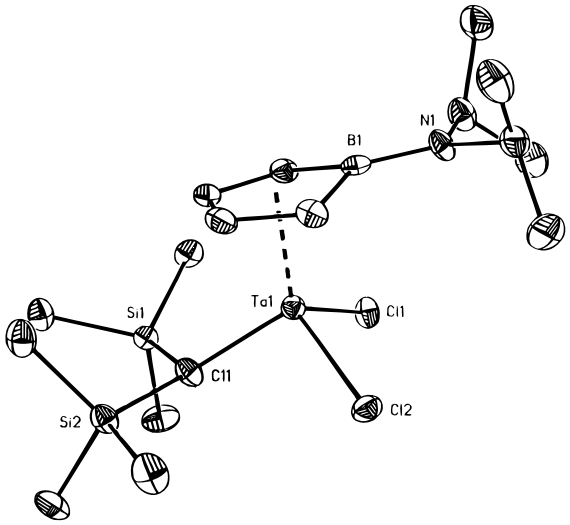

Figure 2. ORTEP drawing of **3** shown at 30% probability. Hydrogen atoms are not shown.

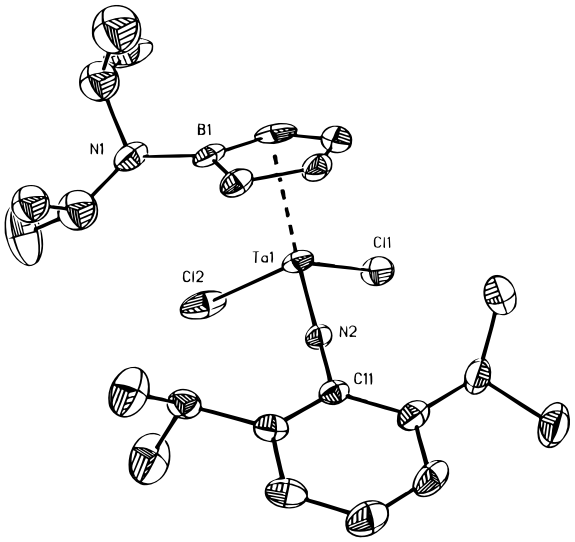

Figure 3. ORTEP drawing of **4** shown at 30% probability. Hydrogen atoms are not shown.

solvents. The ^{1}H NMR characteristics of the α-hydrogen in **3** are unusual. H_α resonates at 3.74 ppm, significantly downfield from the resonances observed for other alkyl complexes. Coupling between C_α and H_α is weak (J_{CH} = 95 Hz), suggesting that H_α interacts either with the metal or with the exocyclic nitrogen on the borollide ring. A single-crystal diffraction study of **3** (Figure 2) shows that the sum of the non-hydrogen angles for C_α (designated C_{11} in Figure 2) is 351.1° and that the Ta−C_α bond distance is short (2.110(8) Å). The orientation of substituents on C_α precludes any interaction between H_α and the exocyclic amine site. These structural parameters are consistent with the presence of an agostic interaction in the solid state, as shown in Scheme 1, which is maintained in solution.

Imido Complexes. Imido ligands (formally, NR^{2-})[29] have received considerable attention recently in view of their ability to stabilize high oxidation state catalysts.[30] Donation of the nitrogen lone-pair to an electron-deficient metal center renders the imido ligand a six-electron donor. Isolobal similarities between imido and cyclopentadienyl complexes have also been noted.[31] Compound **1** is a logical starting material for the syntheses of borollide−imido complexes. For this purpose we chose the bulky diisopropylphenylimido fragment since it is well-known to favor formation of mononuclear complexes.[12a]

Addition of H_2NAr (Ar = 2,6-^{i}Pr$_2$-C$_6$H$_3$) to **1** in benzene, followed by treatment with 2 equiv of triethylamine and extraction with pentane gives a single product (**4**) for which ^{1}H NMR spectroscopy shows to contain a *protonated* nitrogen functionality. The IR spectrum of **4** shows a band at 1347 cm^{-1} which is in the range for terminal imido ligands. A single-crystal diffraction study (Figure 3) reveals that the exocyclic nitrogen is sp^3 hybridized and that the B−N distance is long (1.556(12) Å) relative to **1** or **3**. The Ta−N−C angle in the imido group of **4** is nearly linear (170.0(6)°) and the Ta−N distance is short (1.778(7) Å). These metrical parameters indicate a formal Ta−N triple bond between tantalum and the imido nitrogen.[29] Indeed, the quasi linear Ta−NAr functionality

(29) Nugent, W. A.; Mayer, J. A. *Metal−Ligand Multiple Bonds*; Wiley-Interscience: New York, 1988.

(30) (a) Walsh, P. J.; Hollander, F. J.; Bergman, R. G. *J. Am. Chem. Soc.* **1988**, *110*, 8729. (b) Cummins, C. C.; Baxter, S. M.; Wolczanski, P. T. *J. Am. Chem. Soc.* **1988**, *110*, 8731. (c) Cummins, C. C.; Schaller, C. P.; Van Duyne, G. D.; Wolczanski, P. T.; Chan, A. W. E.; Hoffman, R. *J. Am. Chem. Soc.* **1991**, *113*, 2985. (d) Schrock, R. R. *Acc. Chem. Res.* **1990**, *23*, 158.

(31) Williams, D. N.; Mitchell, J. P.; Poole, A. D.; Siemeling, U.; Clegg, W.; Hockless, D. C. R.; O'Neil, P. A.; Gibson, V. C. *J. Chem. Soc., Dalton Trans.* **1992**, 739.

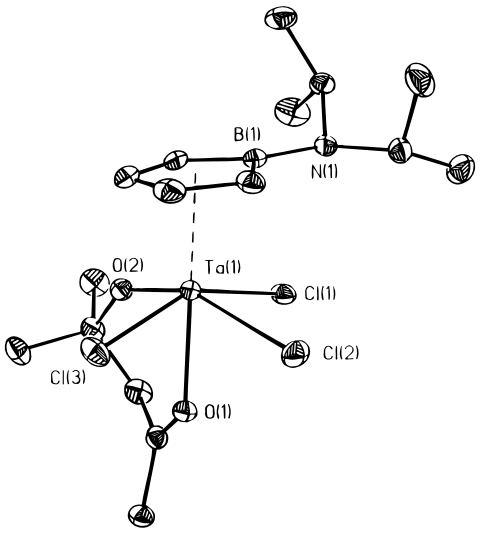

Figure 4. ORTEP drawing of **5** shown at 30% probability. Hydrogen atoms are not shown.

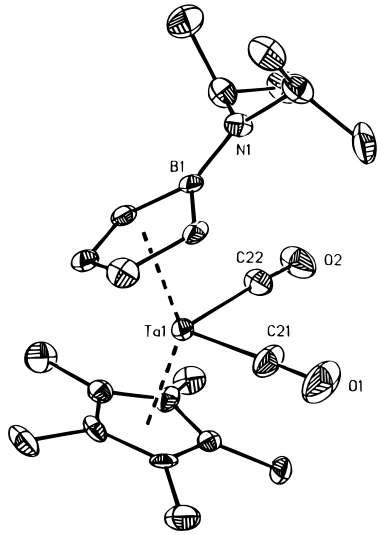

Figure 5. ORTEP drawing of **7** shown at 30% probability. Hydrogen atoms are not shown.

in **4** is nearly isostructural to that observed in the isoelectronic counterpart, Cp*$TaCl_2$(NAr) (d(Ta−N) = 1.780(5) Å, Ta−N−C = 171.4(5)°).[31] Product **4** adopts the zwitterionic structure shown in Scheme 1.

Heterolytic C−H Bond Activation. Addition of 2 equiv of anhydrous acetone to **1** results in the formation of orange [C_4H_4B-NH(CHMe_2)$_2$]$TaCl_3$[Me_2C(O)CH_2C(O)Me] (**5**) as shown in Scheme 1. Diagnostic ^{1}H NMR data include a signal at 1.06 ppm corresponding to *two* methyl groups and a peak at 1.69 ppm from the methyl group adjacent to the bound carbonyl functionality.

A crystal structure determination (Figure 4) revealed that the overall geometry of **5** is pseudo-octahedral and confirmed the presence of a protonated nitrogen (d(B−N) = 1.554(6) Å). Of particular importance are the short bond between Ta and the alkoxide oxygen (d(Ta−O(2)) = 1.888(3) Å) and the long bond to the coordinated ketone (d(Ta−O(2)) = 2.257(3) Å). Distinguishable C−O single (d(O(2)−C(14) = 1.428(5) Å) and C═O double bonds (d(O(1)−C(11) = 1.220(5) Å) are also evident. Compound **5** can also be prepared directly from **1** and 1 equiv of 4-hydroxy-4-methyl-2-pentanone (diacetone alcohol).

Diacetone alcohol is the product of the aldol condensation of acetone, which can be catalyzed by Lewis acids. Floriani has structurally characterized several early transition metal complexes of the products.[32,33] Based on this mechanistic work, we propose the sequence of steps shown in Scheme 2 for the formation of **5**.[34]

Coordination of acetone is followed by deprotonation of one methyl group by the exocyclic nitrogen. A second equiv of acetone coordinates and undergoes attack by the enolate carbon, resulting in carbon−carbon bond formation. Alternatively, coordination of both acetone molecules precedes deprotonation and nucleophilic attack.

Synthesis of Metallocene Mimics. Much of the interest in studying electrophilic complexes containing boron heterocycles stems from the potential for preparing new molecules with attributes similar to group 4 metallocenes. The number of tantalocene mimics containing borollide ligands in the literature is limited, probably because of the multistep synthesis of the requisite starting material, Cp*$TaMe_2Cl(OSO_2CF_3)$.[4] Introduction of co-ligands other than Cp* is not achievable under this methodology, severely limiting the range of compounds available.

Scheme 2

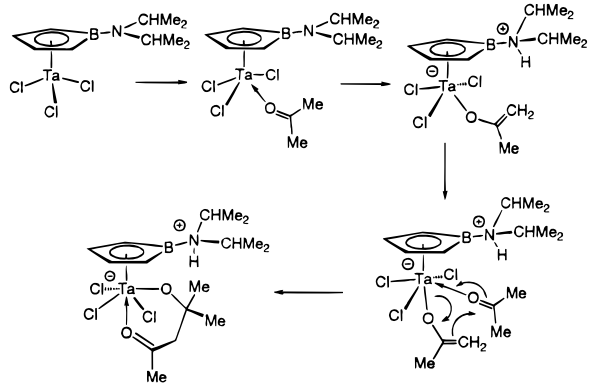

We have found that **1** can be used to prepare a wide range of metallocene mimics. For example, reaction of Cp*Li with **1** gives green Cp*[C_4H_4B-N(CHMe_2)$_2$]$TaCl_2$ (**6**) in 75% yield (Scheme 3). The new procedure for **6** represents a significant improvement over the previous method, which requires photolytic conversion of Cp*[C_4H_4B-N(CHMe_2)$_2$]$TaMe_2$ in chloroform.[4]

Magnesium reduction of **6** in THF under an atmosphere of CO gives the air stable product Cp*[C_4H_4B-N(CHMe_2)$_2$]Ta(CO)$_2$ (**7**, as shown in Scheme 3). The molecular structure of **7**, shown in Figure 5, shows a rare example of low valent Ta bound to borollide. The CO stretching frequencies of 1969 and 1894 cm^{-1} for **7** in CH_2Cl_2 are in the range observed for Cp_2Zr(CO)$_2$ (ν_{CO} = 1975 and 1886 cm^{-1}, compare with ν_{CO} = 2143 cm^{-1} for free CO).[35] Protonation of **7** with [H(OEt_2)$_2$][B(C_6H_3(CF_3)$_2$)$_4$][36] in methylene chloride gives {[C_4H_4B-NH(CHMe_2)$_2$]Cp*Ta(CO)$_2$}{[B(C_6H_3(CF_3)$_2$)$_4$]}(**8**) as the exclusive

(32) Veya, P.; Cozzi, P. G.; Floriani, C.; Rotzinger, F. P.; Chiesi-Villa, A.; Rizzoli, C. *Organometallics* **1995**, *14*, 4101.

(33) Cozzi, P. G.; Veya, P.; Floriani, C.; Rotzinger, F. P.; Chiesi-Villa, A.; Rizzoli, C. *Organometallics* **1995**, *14*, 4092.

(34) Early transition metal complexes are known to affect the reactivity patterns of enolates: Paterson, I. In *Comprehensive Organic Synthesis*; Heathcock, C. H., Ed.; Pergamon Press: Oxford, 1991; Vol. 1, p 301.

(35) Demerseman, B.; Bouguet, G.; Bigorgne, M. *J. Organomet. Chem.* **1977**, *132*, 223.

(36) Brookhart, M.; Grant, B.; Volpe, A. F., Jr. *Organometallics* **1992**, *11*, 3920.

Scheme 3[a]

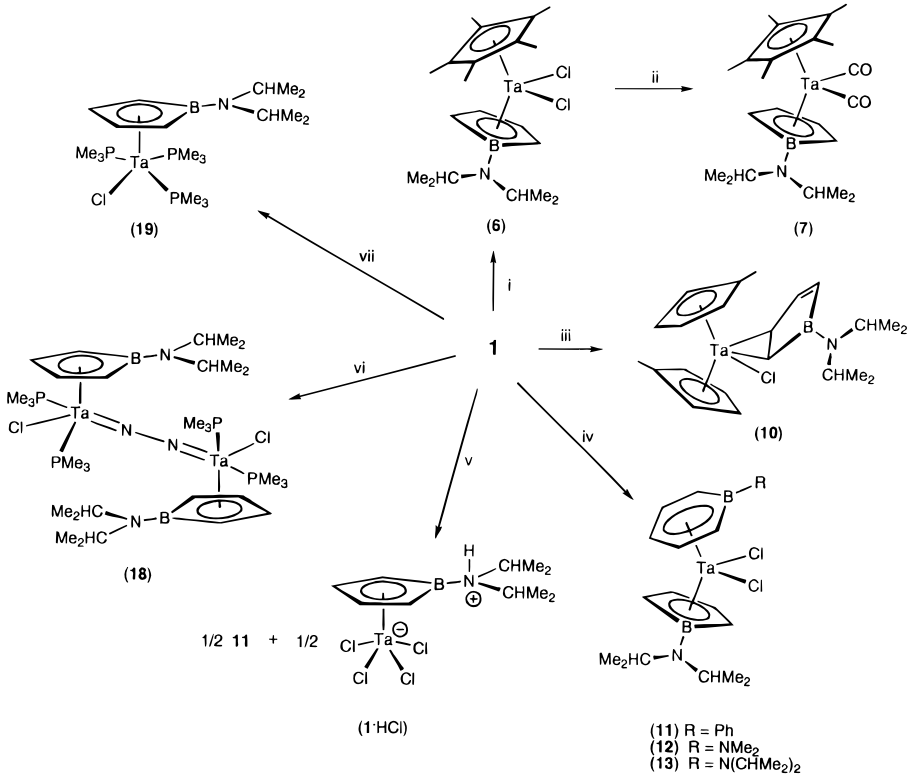

[a] (i) 1.0 equiv of LiCp*, THF, −35 °C; (ii) Mg, CO, THF, − 78 °C; (iii) excess LiCp′, THF, room temperature; (iv) 1.0 equiv of Li[C_5H_5B-R] (R = Ph, NMe_2, or $N(CHMe_2)_2$), Et_2O, −35 °C; (v) 0.5 equiv of C_5H_6B-Ph, C_6H_6, room temperature; (vi) Mg, excess PMe_3, N_2, THF, −78 °C; (vii) Mg, excess PMe_3, Ar, THF, −78 °C.

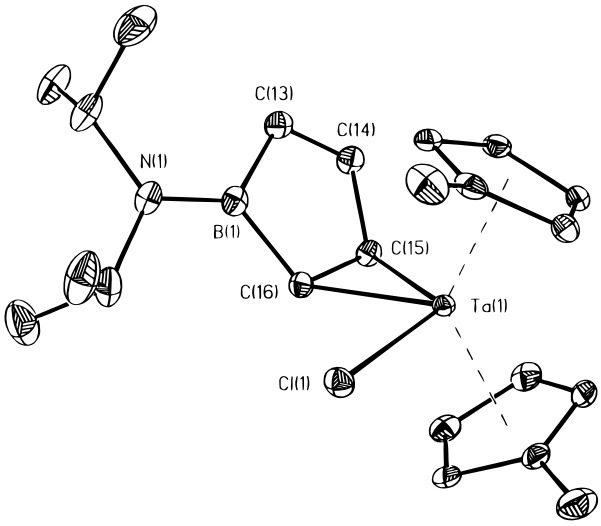

Figure 6. ORTEP drawing of **10** shown at 30% probability. Hydrogen atoms are not shown.

product by ^{1}H NMR spectroscopy. The CO stretching frequencies for **8** (2000 and 1899 cm^{-1}) are considerably higher than those of **7**. The reduction in back-bonding from tantalum to CO provides spectroscopic proof of a shift in electron density from tantalum to boron.

The green complex Cp′[C_4H_4B-$N(CHMe_2)_2$]$TaCl_2$ (**9**, Cp′ = C_5H_4Me) can also be prepared via treatment of **1** with 1 equiv of Cp′Li. Compound **9** reacts with an additional equiv of Cp′Li to form orange Cp′$_2$[η^2-C_4H_4B-$N(CHMe_2)_2$]TaCl (**10**, in Scheme 3). A single-crystal diffraction study (Figure 6) reveals **10** to be the first example of an η^2-borole ligand bound to a transition metal. The long C(15)−C(16) bond distance (1.464(6) Å) indicates significant back-bonding to the borole double-bond.[37] For comparison, note that the C(13)−C(14) distance is 1.347(6) Å. It is known that oxidation of [C_4H_4B-$N(CHMe_2)_2$]$^{2-}$ leads to the formation of the neutral borole [C_4H_4B-$N(CHMe_2)_2$] which quickly dimerizes via a Diels−Alder reaction.[24] The stabilization of the highly reactive borole by "Cp′$_2$TaCl" is thus analogous to the formal trapping of benzyne[38] by "Cp_2Zr" in $Cp_2Zr(C_6H_4)(PMe_3)$.[38c]

At room temperature, the two Cp′ ligands in **10** are inequivalent by ^{1}H NMR spectroscopy. At 49 °C, the two methyl resonances coalesce, corresponding to an activation energy of 16.1 ± 0.5 kcal/mol. A plausible mechanism for equilibration of the two Cp′ ligands involves a hapticity change of the borollide ligand from η^2 to η^5 as shown below. This fluxional process does not average the two sides of each Cp′ ligand, consistent with experimental observations.[39] As drawn, the proposed intermediate is a 20 electron complex. An η^5-to-η^3 shift on one of the Cp′ ligands would maintain an 18 electron configuration.

Addition of Li[C_5H_5B-Ph] or Li[C_5H_5B-NMe_2] to **1** results in the formation of [C_4H_4B-$N(CHMe_2)_2$][C_5H_5B-Ph]$TaCl_2$ (**11**) or [C_4H_4B-$N(CHMe_2)_2$][C_5H_5B-NMe_2]$TaCl_2$ (**12**), respectively (Scheme 3). Alternatively the boratabenzene salt can be formed in situ. For example, [C_4H_4B-$N(CHMe_2)_2$][C_5H_5B-

(37) For other olefin type coordination to tantalum, see: McDade, C.; Gibson, V. C.; Santarsiero, B. D.; Bercaw, J. E. *Organometallics*, **1988**, *7*, 1.

(38) See, for example: (a) McLain, S. J.; Schrock, R. R.; Sharp, P. R.; Churchill, M. R.; Youngs, W. J. *J. Am. Chem. Soc.* **1979**, *101*, 263. (b) Bennett, M. A.; Hambley, T. W.; Roberts, N. K.; Robertson, G. B. *Organometallics* **1985**, *4*, 1992. (c) Buchwald, S. L.; Watson, B. T.; Huffman, J. C. *J. Am. Chem. Soc.* **1986**, *108*, 7411. (d) Buchwald, S. L.; Nielsen, R. B. *Chem. Rev.* **1988**, *88*, 1047.

(39) See: Elschenbroich, C.; Salzer, A. *Organometallics;* VCH: New York, 1989.

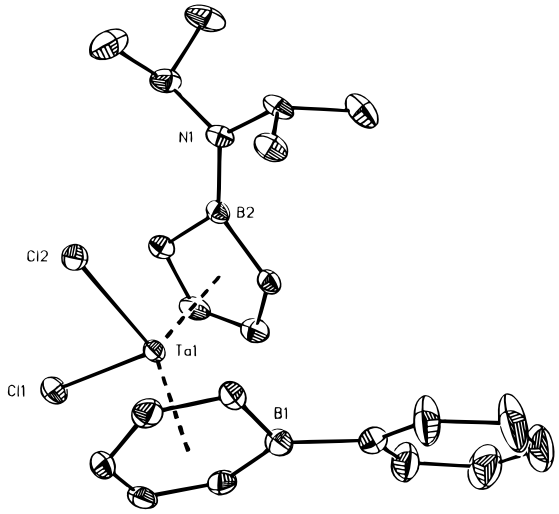

Figure 7. ORTEP drawing of **11** shown at 30% probability. Hydrogen atoms are not shown.

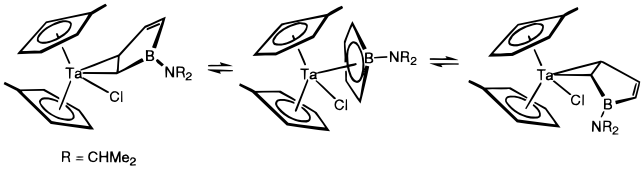

$N(CHMe_2)_2]TaCl_2$ (**13**) was prepared by mixing $[C_5H_6B$-$N(CHMe_2)_2]$ and LDA (LDA = lithium diisopropylamide) and adding the resulting solution to **1**. This approach circumvents the isolation of discrete lithium salts which can be of low yield. Complexes **11**−**13** are the first examples of metallocene-like molecules supported by a combination of boratacyclic ligands. The molecular structures of **11** and **12**, as determined by X-ray crystallography, resemble the geometry of group 4 bent metallocenes (Figures 7 and 8, respectively).

In the absence of a strong base, **1** may serve as a deprotonating reagent. Thus, when 2 equiv of **1** are mixed with $[C_5H_6B$-Ph] over a period of 8 days at room temperature, one obtains zwitterionic $[C_4H_4B$-$NH(CHMe_2)_2]TaCl_4$ (**1**·HCl) and **11** as the products (Scheme 3). Complex **1**·HCl can also be obtained quantitatively by treating **1** with excess HCl.

There are subtle differences in the way that the boratabenzene ligand in **11** and **12** interact with the metal relative to the binding observed in the isoelectronic $[C_5H_5B$-$N(CHMe_2)_2]_2ZrCl_2$ molecule. In both **11** and **12** the bond distances between Ta and the five boratabenzene carbon atoms are nearly identical. The distortion toward η^5-pentadienyl coordination is not as pronounced as that observed in $[C_5H_5B$-$N(CHMe_2)_2]_2ZrCl_2$.[9a] It appears that the presence of the aminoborollide co-ligand and the resulting low-valent resonance contribution strengthen the interaction between the metal and the boron atom in the boratabenzene fragment, thus favoring η^6 coordination. For both **11** and **12** the average distance from Ta to the borollide carbons is shorter (in Å: $d(\mathrm{Ta-C_{ave}}_{\mathbf{11}}) = 2.36(1)$, $d(\mathrm{Ta-C_{ave}}_{\mathbf{12}}) = 2.36(1)$) than the average Ta−C distances of the boratabenzene ligand (in Å: $d(\mathrm{Ta-C_{ave}}_{\mathbf{11}}) = 2.48(1)$, $d(\mathrm{Ta-C_{ave}}_{\mathbf{12}}) = 2.47(1)$) as would be expected on the basis of increased Coulombic attraction.

Hydrogenation Reactions of $[C_4H_4B$-$N(CHMe_2)_2][C_5H_5B$-Ph]$TaMe_2$. We recently reported that $Cp^*[C_4H_4B$-$N(CHMe_2)_2]$-$TaMe_2$ reacts with H_2 in the presence of PMe_3 to give $Cp^*[C_4H_4B$-$N(CHMe_2)_2]Ta(H)_2(PMe_3)$.[8] This hydrogenation proceeds more than 3 orders of magnitude faster than analogous reactions with isoelectronic $Cp^*_2ZrMe_2$[40] and was shown to proceed via low valent intermediates which could be trapped with excess PMe_3. In neat PMe_3, the reaction exclusively gives $Cp^*[C_4H_4B$-$N(CHMe_2)_2]Ta(PMe_3)_2$ and 2 equiv of methane. Understanding this hydrogenation reaction provides insight into the effect of boratacyclic ligands on the mechanisms of elementary reactions. With the availability of **11** and **12** in good quantities it should be possible to examine the effect of boratabenzene for Cp* substitution on the outcome of these hydrogenation processes.

Methylation of **11** or **12** proceeds cleanly using 2 equiv of MeLi in diethyl ether, forming $[C_4H_4B$-$N(CHMe_2)_2][C_5H_5B$-$Ph]TaMe_2$ (**14**) (eq 2) or $[C_4H_4B$-$N(CHMe_2)_2][C_5H_5B$-$NMe_2]$-$TaMe_2$ (**15**), respectively.

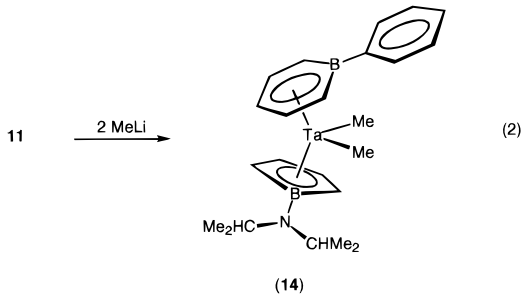

Methane generation and a color change from blue to orange-yellow are observed when a C_6D_6 solution of **14** is treated with 620 Torr H_2 in the presence of 2 equiv of PMe_3. The product of the reaction is $[C_4H_4B$-$N(CHMe_2)_2][C_5H_5B$-$Ph]Ta(PMe_3)_2$ (**16**) as shown in eq 3. Neither intermediates nor the expected hydride product were observed when the reaction was monitored by ^{1}H NMR spectroscopy. Cooling a pentane solution of **16** to −30 °C gave crystals suitable for crystallography, and the results of this study are shown in Figure 9. The overall molecular structure of **16** is similar to that of the previously characterized $Cp^*[C_4H_4B$-$N(CHMe_2)_2]Ta(PMe_3)_2$.[8]

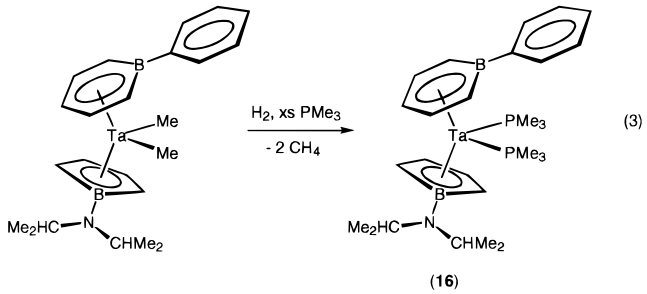

Reaction of **14** with 2 equiv of PEt_3 and 604 Torr H_2 for 5 days gives the dihydride product, *trans*-$[C_4H_4B$-$N(CHMe_2)_2]$-$[C_5H_5B$-Ph]$Ta(PEt_3)H_2$ (**17** in eq 4). The X-ray crystal structure of **17** is shown in Figure 10. The hydrides were located and refined, revealing Ta−H bond distances of 1.659(5) Å and 1.746(5) Å. One hydride is in close proximity to the boron of the boratabenzene ring ($d(B_1-H_2) = 1.862(5)$ Å), and the phosphorus atom is not at the center of the wedge, as in Cp^*-$[C_4H_4B$-$N(CHMe_2)_2]Ta(H)_2(PMe_3)$, but rather at an angle of 10.0(5)° from the centroid−Ta−centroid plane. These parameters, in conjunction with the Ta−H_2−B_1 angle of 89.6°, suggest

(40) (a) Miller, F. D.; Sanner, R. D. *Organometallics* **1988**, *7*, 818. (b) Lin, Z.; Marks, T. J. *J. Am. Chem. Soc.* **1987**, *109*, 7979. (c) Jordan, R. F.; Bajgur, C. S.; Dasher, W. E.; Rheingold, A. L. *Organometallics* **1987**, *6*, 1041.

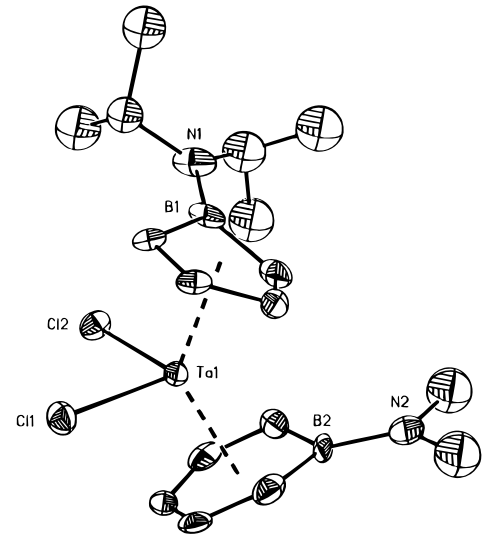

Figure 8. ORTEP drawing of **12** shown at 30% probability.

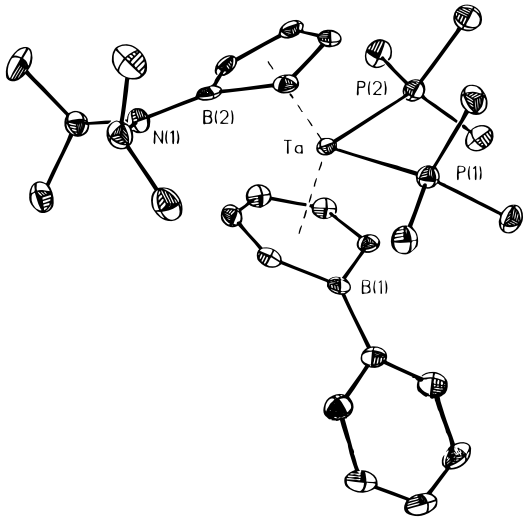

Figure 9. ORTEP drawing of **16** shown at 30% probability. Hydrogen atoms are not shown.

a Ta−H−B three-centered interaction.[41] The ^{11}B NMR spectrum of **17** shows two signals at 33.7 and 19.4 ppm. The upfield shift of the boratabenzene boron atom to 19.4 ppm has been attributed to the Ta−H−B three-centered interaction (compare against 35.0 ppm for **14**).[41a]

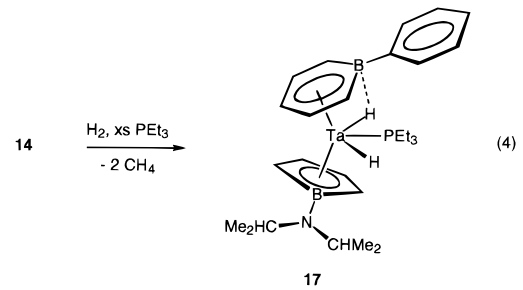

Different hydride environments are confirmed by the low temperature ^{1}H NMR spectra of **17**. At room temperature, the doublet representative of the averaged hydrides has a J_{PH} of 59.5 Hz and is centered at −2.75 ppm. Upon lowering the temperature the static spectrum is observed with different J_{PH} values and chemical shifts (−2.05 ppm; J_{PH} = 38 Hz and −3.80 ppm; J_{PH} = 70 Hz) (Figure 11).

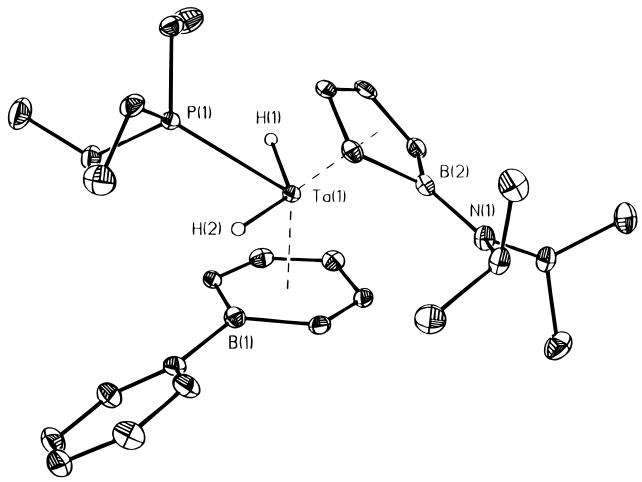

Figure 10. ORTEP drawing of **17** shown at 30% probability. Hydrogen atoms are not shown.

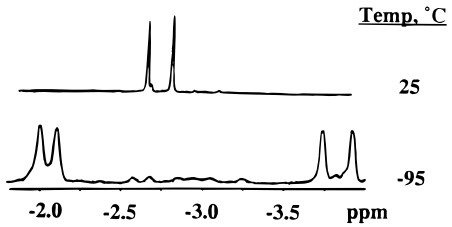

Figure 11. High and low temperature ^{1}H NMR spectra for the hydride signals of **17**.

Reduction Reactions

The versatile substitution chemistry of **1** prompted us to investigate whether dianionic ligands, such as tribenzylideneemethane, $[C(CHPh)_3]^{2-}$,[42] or borollide could be exchanged for chloride ligands. Our initial goal was to explore the possibility of creating metallocene-like environments supported by two dianionic Cp mimics.[43]

The reaction of **1** with 1 equiv of $Li_2[C_4H_4B\text{-}N(CHMe_2)_2]\cdot$THF in THF in the presence of excess PMe_3 results in the formation of an orange product. ^{1}H and ^{13}C NMR spectroscopy indicate that this product contains one borollide and two PMe_3 ligands. Reproduction of this reaction using $Li_2[C(CHPh)_3](TMEDA)_2$ instead of borollide gives the same product. Apparently, the dianions simply act as reducing agents. To confirm this, **1** was treated with Mg in the presence of PMe_3, and the same product was formed. X-ray crystallography shows that this product is the μ-dinitrogen complex, $\{[C_4H_4B\text{-}N(CHMe_2)_2](Me_3P)_2ClTaN\}_2$ (**18**), as shown in Scheme 3.

The ORTEP diagram of **18** is shown in Figure 12. The Ta−N bond distances are short (d(Ta−N(3)), 1.838(7) Å; d(Ta−N(4)), 1.838(7) Å), and the N−N bond distance of 1.309(9) Å is longer than that of free N_2 (1.0976 Å).[44] These metrical parameters are directly comparable to those observed in [Ta-

(41) (a) Herberich, G. E.; Carstensen, T.; Köffer, D. P. J.; Klaff, N.; Boese, R.; Hyla-Kryspin, I.; Gleiter, R.; Stephan, M.; Meth, H.; Zenneck, U. *Organometallics* **1994**, *13*, 619. (b) Herberich, G. E.; Hessner, B.; D. Köffer, D. P. J. *J. Organomet. Chem.* **1989**, *362*, 243.

(42) Rodriguez, G.; Bazan, G. C. *J. Am. Chem. Soc.* **1995** *117*, 10155.

(43) This has been accomplished using dicarbollide ligands. (a) Manning, M. J.; Knobler, C. B.; Khattar, R.; Hawthorne, M. F. *Inorg. Chem.* **1991**, *30*, 2009. (b) Gomez, F. A.; Johnson, S. E.; Knobler, C. B.; Hawthorne, M. F. *Inorg. Chem.* **1992**, *31*, 3558.

(44) For a review of dinitrogen complexes, see: Hidai, M.; Mizobe, Y. *Chem. Rev.* **1995**, *95*, 1115.

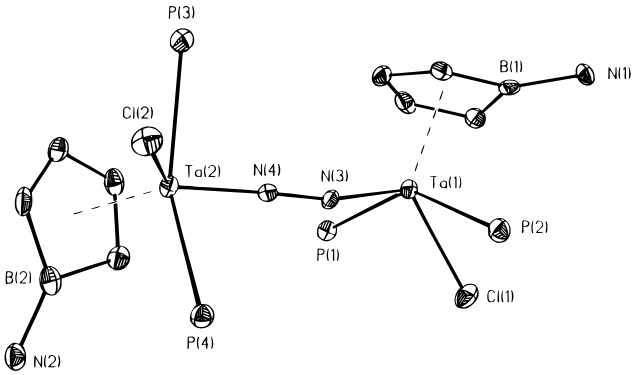

Figure 12. ORTEP drawing of **18** shown at 30% probability. Diisopropyl and methyl groups have been omitted for clarity. Hydrogen atoms are not shown.

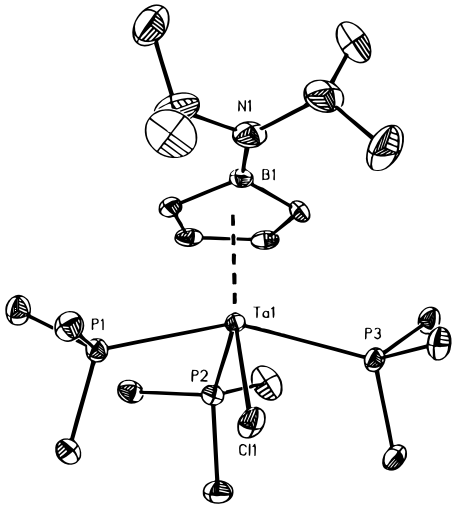

Figure 13. ORTEP drawing of **19** shown at 30% probability. Hydrogen atoms are not shown.

$(CHCMe_3)(PMe_3)_2(CH_2CMe_3)])_2(\mu\text{-}N_2)$ (d(Ta−N), 1.84 Å; d(N(1)−N(2)), 1.298 Å).[45] The dinitrogen fragment binds to the metal in a hydrazido(4−), diimido fashion,[46] and is bonded in a largely linear manner ((Ta═N−N) = 167.8(7)°). Complex **18** is inert to N_2 displacement (with acetone), chloride abstraction (with Ag^+), and chloride metathesis (with lithium amides and alkyls).

Reduction of **1** under argon rather than nitrogen leads to the formation and isolation of a different complex, the mononuclear $[C_4H_4B\text{-}N(CHMe_2)_2]Ta(PMe_3)_3Cl$ (**19**) (Scheme 3). Upon exposure to nitrogen, **19** reacts immediately to form **18**. Complex **19** is highly reactive with even small amounts of N_2 at low temperatures, preventing a detailed study of the conversion from **19** to **18**. The X-ray crystal structure of **19** (Figure 13) shows an unexceptional four-legged piano stool geometry with the borollide fragment rotated such that steric contacts between the diisopropyl groups and the bulky PMe_3 ligands are minimized. Overall, the formation of **18** from **19** parallels the reactions of $Ta(C_2H_4)(PMe_3)_4Cl$ and $Ta(CHCMe_3)(PMe_3)Cl$ with N_2 which give $[Ta(C_2H_4)(PMe_3)_3Cl]_2(\mu\text{-}N_2)$ and $[Ta(CHCMe_3)(PMe_3)_3Cl]_2(\mu\text{-}N_2)$, respectively.[45]

The reaction of **19** with H_2 proceeds cleanly by ^{1}H NMR spectroscopy. At room temperature the product contains two inequivalent borollide rings, two hydride ligands which appear as complex patterns (^{1}H NMR: δ 7.61 H_a; −2.78 H_b) and three phosphine ligands ($^{31}P\{^1H\}$ NMR δ: −5.1, P_1, J_{P1P3} = 53.1 Hz; −6.6 P_2, J_{P2P3} = 7.1 Hz; −10.6, P_3; J_{P1P3} = 53.2 Hz, J_{P2P3} = 6.9 Hz). The two hydride signals are not coupled to each other. Each shows *strong* coupling to one phosphine (in Hz: J_{P2Ha} = 72.9; J_{P3Hb} = 28.2) and considerably weaker coupling to the other two phosphines (in Hz: J_{P3Ha} = 12.8, J_{P1Ha} < 5, J_{P2Hb} < 5, J_{P1Hb} < 3), as shown by selective $^1H\{^{31}P\}$ NMR spectra.

(45) Rocklage, S. M.; Turner, H. W.; Fellmann, J. D.; Schrock, R. R. *Organometallics* **1982**, *1*, 703.

(46) Rocklage, S. M.; Schrock, R. R. *J. Am. Chem. Soc.* **1982**, *104*, 3077.

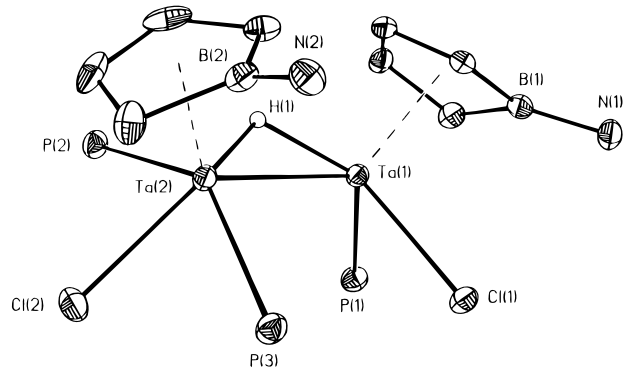

Figure 14. ORTEP drawing of **20** shown at 30% probability. Diisopropyl and methyl groups have been omitted for clarity. Hydrogen atoms are not shown.

Since these data do not allow for an unambiguous assignment, the solid state structure was determined crystallographically, and the results of this study are shown in Figure 14. The overall molecular geometry contains two nonequivalent tantalum atoms at a distance of 2.9460(3) Å from each other. In addition to a borollide ligand, Ta(1) contains one chloride and one phosphine ligand, while Ta(2) contains one chloride and two phosphine ligands. The location of the two hydrides is more difficult to assign. One hydride was located in the electron density map adjacent to the two tantalum atoms and was assigned as the bridging hydride. The second hydride was not reliably located. Note that the Cl−Ta−P angles are nearly identical for both metal centers (in °, Cl(1)−Ta(1)-P(1) = 76.24(5), Cl(2)−Ta-(2)-P(2) = 72.6(6), Cl(2)−Ta(2)-P(3) = 73.32(6)), and therefore there appears to be a ligand missing on Ta(1) at the site pseudotrans from Cl(1). We assume that this site is occupied by a terminal hydride and therefore propose that addition of H_2 to **19** gives $([C_4H_4B\text{-}N(CHMe_2)_2]Ta(H)(PMe_3)Cl)\mu\text{-}H([C_4H_4B\text{-}N(CHMe_2)_2]Ta(PMe_3)_2Cl)$ (**20**) as shown in eq 5.

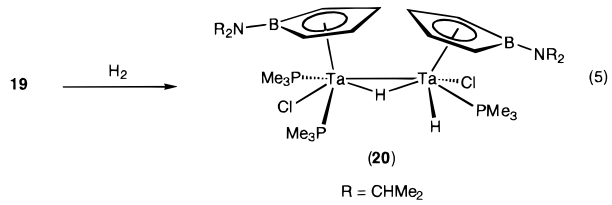

Summary and Conclusion

Treating $AlCl_3$ with $Li_2[C_4H_4B\text{-}N(CHMe_2)_2]\cdot$THF attenuates the propensity of the borollide dianion to participate in reduction reactions and allows for the synthesis of **1**. Although the mechanism is poorly understood at the present time, the reaction is reliable and amenable to scale-up. The versatile substitution chemistry of **1**, in turn, provides an unprecedented opportunity to prepare and examine the properties of borollide−tantalum complexes of various oxidation states and with different co-ligands.

While **1** is isoelectronic to Cp^*ZrCl_3 and $CpZrCl_3$, alkylation reactions proceed differently. The higher electron density at

borollide, relative to cyclopentadienyl, makes it a better bridging ligand and is probably responsible for the formation of **2** (Scheme 1),[47] a remarkably electron deficient (24 electron) triple decker complex.[48] The C−H agostic interaction in **3** and the imido ligand formation in zwitterionic **4** are driven by the electron demand at tantalum.[49] The weaker Ta−C double bond and the less acidic C−H bond combine to preclude alkylidene formation from **3**. Precoordination of acetone is probably required prior to C−H activation and the formation of **5** is a result of the close proximity of the Lewis acidic metal site and the Lewis basic amine functionality. The prospects of effecting heterolytic activations of this type have been discussed previously.[3]

Thus far, the substitution reactions of **1** provide the most convenient and general entry into tantalum−borollide metallocene mimics. Despite the structural and electronic similarities to group 4 metallocenes, the borollide−tantalum complexes have failed to generate olefin polymerization catalysts with competitive reactivity. The general reactivity profile of these complexes suggests that the Ta−CH_3 bond is less polar, at least within this general coordination sphere, than the M−CH_3 bond (M = Ti, Zr, Hf) in standard metallocenes and is therefore more difficult to activate for olefin insertion chemistry.

The dicarbonyl complex **7** and its protonated analogue **8** provide the opportunity to gauge the changes in electron density at the metal upon changing the character of the exocyclic boron substitutent by inspection of their corresponding carbonyl stretching frequencies. The increase from 1969 and 1894 cm^{-1} in **7** to 2000 and 1899 cm^{-1} in **8** clearly demonstrates weaker Ta−CO back-bonding. Disruption of B−N π bonding results in removal of electron density from the metal and minimizes the contribution from resonance structures **B** and **C**. Despite this information, it is still unclear whether boron serves as a better conduit than carbon for transferring electron density from exocyclic groups to the metal. A comparison of complexes such as Cp*[$C_5H_4NR_2$]Zr(CO)$_2$ and [Cp*[$C_5H_4NHR_2$]Zr(CO)$_2$]X (X = noncoordinating counteranion) would be helpful in this respect.

The synthesis and characterization of **10** demonstrate that borollide can bind in an η^2-fashion to transition metals and that, under some conditions, it can undergo η^2-to-η^5 hapticity changes. This behavior is analogous to the η^5-to-η^3 ring slippage which has been observed for the cyclopentadienyl ligand.[39] Similarly, compounds **11**−**13** provide for the first time access into the chemistry of metallocene mimics supported by different boratacycles.

Structural and spectroscopic characterization of **17** shows that the electrophilic boron atom can interact with hydride ligands thereby affecting their properties. Precedent for three-center two-electron interactions of this type exists in iron−borollide hydrides such as CpFeH(C_4H_4B-Ph).[41] No ^{11}B−^{1}H coupling is observed in either type of complex. The three-center two-electron interaction enhances the borate nature of the boratabenzene boron and allows the metal to slip to the back of the ring and bind in a pentadienyl fashion.

Reduction of **1** with magnesium in the presence of PMe_3 gives the dinitrogen complex **18** or mononuclear **19** depending on whether the reaction is exposed to nitrogen or argon. When **19** is treated with hydrogen, the mixed-valent dinuclear complex **20** is obtained. It is significant that only one-half equiv of H_2 is activated per tantalum. Our explanation for the formation and structure of **20** is based on a Lewis-acid−Lewis-base pairing as shown below. In this interpretation, a formally high valent [C_4H_4B-N($CHMe_2$)$_2$]TaCl(H)$_2$$PMe_3$ combines with a low valent [C_4H_4B-N($CHMe_2$)$_2$]TaCl(PMe_3) fragment to form a dative bond between the two metal centers. One of the hydride ligands then bridges the two metal sites.

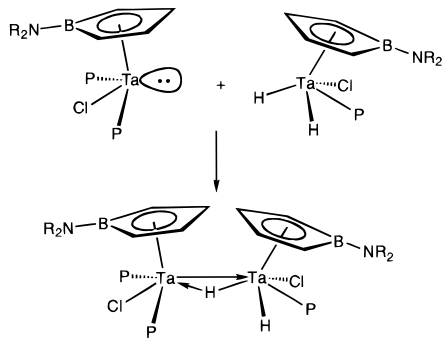

Finally, structural characterization of the range of complexes presented in this paper provides an excellent opportunity to examine how tantalum−borollide bonding adjusts as a function of co-ligands and oxidation states. In particular, the relative contributions of the canonical forms **A**, **B**, and **C** to the electronic structure of a particular complex may be inferred from patterns in tantalum−carbon and tantalum−boron bond distances. Because the tantalum centers are formally ambivalent, even a qualitative measure of the relative importance of these resonance structures conveys important information about the electron density at Ta within a particular ligand environment.

Relevant metrical data are summarized in Tables 1 and 2. Table 1 contains important bond distances for complexes reported in this paper. In all cases containing *unprotonated* [C_4H_4B-N($CHMe_2$)$_2$], the B−N bond lengths are statistically indistinguishable (within 2σ) and compare well to unperturbed B−N double bonds.[50] Resonance structure **A** thus makes only a minimal contribution when B−N π-bonding is possible. The electronic structure is dominated by a combination of **B** and **C**, which may be considered as limiting structures for a substituted *cis*-butadiene complex. The large body of data accumulated in the literature suggests that for these two extreme cases different

Table 2. Average Ta−C Bond Distances and Δ Values for Complexes of [C_4H_4B-N($CHMe_2$)$_2$]

compd no.		d(Ta−C$_\alpha$) (Å)	d(Ta−C$_\beta$) (Å)	Δ (Å)
3		2.320(10)	2.315(10)	0.005(20)
1		2.315(10)	2.306(10)	0.009(20)
12		2.378(13)	2.351(12)	0.027(25)
11		2.377(6)	2.338(7)	0.039(13)
24		2.400(10)	2.340(10)	0.060(20)
17		2.398(4)	2.328(4)	0.070(8)
20	Ta(1)	2.396(6)	2.320(6)	0.076(12)
18		2.423(8)	2.331(8)	0.092(16)
21		2.415(15)	2.315(15)	0.100(30)
22		2.405(10)	2.299(10)	0.107(20)
19		2.369(5)	2.259(5)	0.110(10)
16		2.427(7)	2.306(7)	0.121(14)
23		2.435(10)	2.311(10)	0.124(20)
7		2.413(11)	2.273(12)	0.140(23)
20	Ta(2)	2.467(6)	2.326(6)	0.141(12)

(47) For the synthesis of another borollide triple decker complex, (μ-η^5−C_4H_4BPh)[V(CO)$_4$]$_2$, see: Herberich, G. E.; I. Hausmann, I.; Klaff, N. *Angew. Chem., Int. Ed. Engl.* **1989**, *28*, 319.

(48) Triple-decker complexes typically contain between 30 and 34 valence electrons. For a treatment of their MO schemes, see: Lauher, J. W.; Elian, M.; Summerville, R. H.; Hoffman, R. *J. Am. Chem. Soc.* **1976**, *98*, 3219.

(49) Schrock, R. R. *Acc. Chem. Res.* **1979**, *12*, 98.

(50) A structure search of the Cambridge Structure Database on the B=N fragment revealed a mean distance for this bond of 1.38(4) Å.

M−C bond lengths should be expected.[51] Diene complexes of the late transition metals are thought to assume form **B** in which $d(M-C_\alpha) \geq d(M-C_\beta)$. This trend is maintained for nearly all complexes surveyed, irrespective of the other co-ligands. Electrophilic early transition metal centers adopt form **C** with $d(M-C_\alpha) < d(M-C_\beta)$. The difference between these bond lengths

$$\Delta \equiv d(M-C_\alpha) - d(M-C_\beta)$$

can be on the order of −0.4 to +0.2 Å. Variations in the intraligand C−C bond distances are also, in principle, diagnostic. However, these shorter bonds span a narrower range and are necessarily less sensitive indicators, typically varying by 0.07 Å or less.

Table 2 collects average Ta−C_α and Ta−C_β distances and resulting Δ values for 13 complexes—those reported in this paper, and **21**−**24** which have been reported elsewhere[4,8,52] containing [C_4H_4B-N($CHMe_2$)$_2$], listed in order of increasing Δ.

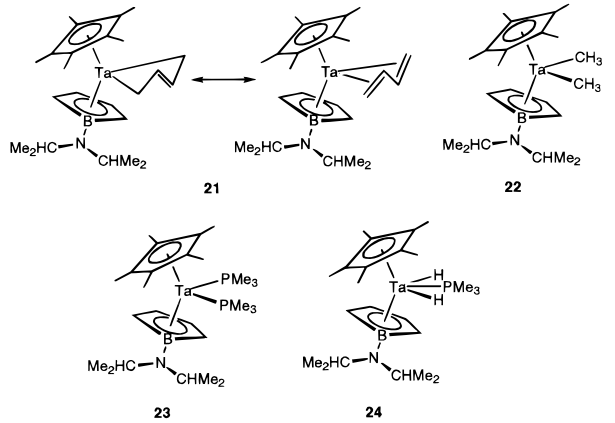

21 **22** **23** **24**

In all cases, Δ is positive. That is, $d(M-C_\alpha) > d(M-C_\beta)$ for all aminoborollide complexes we have studied. If we extend the trends observed for the butadiene ligand to borollide and assume that the boron link does not perturb greatly the ability of the diene fragment to approach the metal, then the data in Table 2 suggest that structure **C** is never a complete description of the ground state. The largest values of Δ in Table 2 are comparable to, or greater than, those observed in late transition metal−diene π-complexes. Analysis of the overall data set suggests that the electronic structure of tantalum−borollide complexes with Δ values above 0.1 Å have a greater contribution by **B**. Those complexes for which Δ is small, the majority of entries in Table 2, probably show strong participation by both **B** and **C**. Most of these tantalum−borollide complexes are therefore best described as possessing metal centers with strongly ambiguous oxidation states.

This conclusion is similar to that reached by Bercaw and coworkers, who argued for the presence of strongly mixed ground states in related borollide complexes of zirconium and hafnium on the basis of evidence from electronic spectroscopy.[5a] Like the tantalum complexes reported here, Cp*[C_5H_4B-N($CHMe_2$)$_2$]M(η^3-C_3H_6) (M = Zr, Hf) are brightly colored. Isostructural substitution of hafnium for zirconium results in a blue shift of ca. 2000 cm^{-1} in the absorption maximum. Because hafnium is more readily oxidized than zirconium, a MLCT transition from a ground-state resembling **B** would have resulted in a red shift. The transition was characterized as having mixed d−d (from the d^2 metal center in structure **B**) and LMCT (from the high-oxidation state structures **A** and **C**) character. The structural data presented here and the spectroscopic argument of Bercaw both suggest that formally electrophilic transition metals bound to borollide should be expected to show chemical characteristics associated with both high and low valency.

Inspection of Table 2 also reveals that complexes with Ta(III)/Ta(I) ambiguity (i.e., **7**, **16**, **19**, **20**, **23**, and perhaps **21**) have statistically greater Δ values than their Ta(V)/Ta(III) counterparts (i.e., **1**, **3**, **11**, **12**, **17**, **18**, **20**, **22**, **24**, and perhaps **21**). This trend is somewhat counterintuitive since increased electron density at the metal should result in more back-bonding to borollide and accentuate the metallacyclopentene form of the ligand.

The utility of the parameter Δ in interpreting structures for which characterization data are incomplete for full assignment may be seen by considering the dinuclear hydride complex **20**, which we have proposed to contain both a high oxidation state and a low oxidation state tantalum. The Ta(V)/Ta(III) center has a Δ value very similar to other phosphine hydride complexes in the series. However, the Ta(III)/Ta(I) center possesses the highest Δ value we have observed, consistent with its low valent description. Analysis of the structural data, in the presence of a large series of related compounds, thus supports the presence of a formal Ta−Ta dative bond in **20**.

Experimental Details

General Considerations. All manipulations were carried out using either high-vacuum or glovebox techniques as previously described.[53] Elemental Analyses were performed by Desert Analytics. ^{1}H, ^{31}P, ^{11}B, and ^{13}C NMR spectra were recorded on a Bruker AMX-400 spectrometer at 400.1 MHz, 161.97 MHz, 128.3 and 100.6 MHz, respectively. The COSY spectrum for **20** was recorded on a QE 300 spectrometer at 300 MHz. Hydrogen and deuterium gases were purchased from Cambridge Isotope Labs. Toluene, benzene, pentane, diethyl ether, and tetrahydrofuran were distilled from benzophenone ketyl. $TaCl_5$, $AlCl_3$, PMe_3, PEt_3, and $P(CHMe_2)_3$ were purchased and used as received from Aldrich. The preparation of Li[C_5H_5-Ph], Li[C_5H_5-NMe_2],[9b,54] and Li_2[C_4H_4B-N($CHMe_2$)$_2$]·THF[25] are available in the literature.

Preparation of [C_4H_4B-N($CHMe_2$)$_2$]$TaCl_3$ (1). A slurry of 1.07 g (8.0 mmol) of $AlCl_3$ in 10 mL of benzene was added slowly to a stirred solution of 1.00 g (4.0 mmol) of Li_2[C_4H_4B-N($CHMe_2$)$_2$]·THF in 20 mL of benzene. The mixture was added to a rapidly stirred suspension of 1.44 g (4.0 mmol) of $TaCl_5$ in 50 mL of benzene, and the resulting purple reaction mixture was allowed to stir for 4 h. The solvent was removed under vacuum, and the product was separated from the green residue by extraction with pentane. The resulting extract was filtered, reduced in volume, and allowed to stand at −35 °C whereupon purple crystals of **1** were deposited. The mother liquor was decanted, and 0.754 g of the product was collected. A second crop of crystals (0.102 g, total yield of 47%) was obtained by reducing the volume of the mother liquor and cooling to −35 °C. ^{1}H NMR (C_6D_6): δ 5.18 (m, 2H, C*H*CHB), 3.91 (m, 2H, CHC*H*B), 3.56 (sept, 2H, C*H*Me_2), 1.09

(51) The Cambridge Structure Database was searched for metallacyclopentene fragments and for transition metals bound in any way to four-carbon fragments with delocalized bonding. From this initial hit set, mononuclear complexes of symmetrically substituted dienes were selected for examination. The search did not give an example of an electrophilic complex with $d(M-C_\alpha) > d(M-C_\beta)$. Substitutents on the diene framework are known to affect significantly the bonding picture (i.e., F substitution strongly favors the metallacyclopentene structure, even at late transition metals). A similar argument has been employed in distinguishing the metallacyclopentene character of a series of *cis*-diene complexes: see ref 5b.

(52) Compound **21** is reported: Sperry, C. K.; Rodriguez, G.; Bazan, G. C. *J. Organomet. Chem.* **1997**, *548*, 1.

(53) Burger, B. J.; Bercaw, J. E. In *Experimental Organometallic Chemistry*; Wayda, A. L., Darensbourg, M. Y., Eds.; ACS Symposium Series 357; American Chemical Society: Washington, D.C., 1987.

(54) Qiao, A.; Hoic, D. A.; Fu, G. C. *J. Am. Chem. Soc.* **1996**, *118*, 8, 6329.

(d, 6H, J = 6.8 Hz, CHMe_2), 1.04 (d, 6H, J = 6.8 Hz, CHMe_2). ^{13}C{^{1}H} NMR (C_6D_6): δ 133.3 (*C*HCHB), 102.0 (br, CH*C*HB), 47.7 (*C*HMe$_2$), 25.1 (CHMe_2), 23.3 (CHMe_2). Elemental Analysis $C_{10}H_{18}BCl_3NTa$, MW = 4504 Calcd: C 26.67, H 4.03, N, 3.11. Found: C 26.73, H 3.97, N 3.07.

Preparation of [C_4H_4B-N(CHMe$_2$)$_2$]TaCl$_2$[CH(SiMe$_3$)$_2$] (3). A slurry of 74 mg (0.44 mmol) of LiCH(SiMe$_3$)$_2$ in 10 mL of benzene was added slowly to a stirred solution of 200 mg (0.44 mmol) of **1** in 5 mL of benzene. The dark olive green solution was allowed to stir for 1 h. The solvent was then removed under vacuum, and the crude product was dissolved in a minimal amount of Et_2O. Upon standing at −35 °C, black crystals of **3** were deposited. The highly soluble product was isolated by rapidly decanting the mother liquor and drying immediately under vacuum (154 mg, 60%). ^{1}H NMR (C_6D_6): δ 5.99 (m, 2H, C*H*CHB), 3.74 (s, 1H, C*H*(SiMe$_3$)$_2$, 3.60 (sept, 2H, C*H*Me$_2$), 3.57 (m, 2H, CHC*H*B), 1.21 (dd, 12H, CHMe_2), 0.10 (s, 18 H, CH(SiMe_3)$_2$). ^{13}C{^{1}H} NMR (C_6D_6): δ 127.1 (*C*HCHB), 114.6 (*C*H(SiMe$_3$)$_2$), 95.6 (CH*C*HB), 47.8 (*C*HMe$_2$), 24.5 (CHMe_2), 22.9 (CHMe_2), 4.5 (CH(SiMe_3)$_2$). Elemental Analysis: $C_{17}H_{37}BCl_2NSi_2Ta$, MW = 574.3, Calcd: C 35.55, H 6.49, N 2.44. Found: C 34.90, H 6.45, N 2.37.

Preparation of [C_4H_4B-NH(CHMe$_2$)$_2$]Ta[N(2,6-(CHMe$_2$)$_2$C$_6$H$_3$)]Cl$_2$ (4). To a solution of **1** (90 mg, 0.20 mmol) in benzene was added H_2N(2,6-(CHMe$_2$)$_2$C$_6$H$_3$) (37.7 μL, 0.20 mmol) dropwise with stirring. A red solution developed. After 5 min, 2 equiv of NEt_3 (55.71 μL, 0.40 mmol) were added dropwise resulting in an orange-yellow solution. This solution was stirred for 10 min before removing solvents under vacuum. The product was extracted with pentane, and the extract was filtered. X-ray quality crystals were obtained from a concentrated pentane solution at −35 °C (yield 91 mg, 78%). ^{1}H NMR (C_6D_6): δ 7.24 (d, 2H, Ar), 6.90 (t, 1H, Ar), 6.25 (m, 2H, C*H*CHB), 5.24 (br, 1H, N*H*), 4.78 (m, 2H, CHC*H*B), 3.90 (sept, 2H, C*H*Me$_2$), 3.00 (sept, 2H, ArC*H*Me$_2$), 1.39 (d, 12H, CHMe_2), 0.74 (d, 6H, Ar(CHMe_2)$_2$), 0.68 (d, 6H, Ar(CHMe_2)$_2$). ^{13}C{^{1}H} NMR (C_6D_6): δ 152.0 (Ar), 145.0 (Ar), 126.4 (Ar), 122.4 (Ar), 122.2 (Ar), 112.7 (*C*HCHB), 98.1 (CH*C*HB), 51.9 (Ar*C*HMe$_2$), 46.7 (*C*HMe$_2$), 22.8 (CHMe_2), 22.3 (CHMe_2), 20.4 (Ar(CHMe_2)$_2$), 19.9 (Ar(CHMe_2)$_2$). FT-IR analysis (in toluene): υ(TaN) = 1347 cm^{-1}. Elemental Analysis: $C_{21}H_{36}BCl_2N_2Ta$, MW = 587.2, Calcd: C 43.53, H 6.22, N 4.84, Cl 12.25. Found: C 44.0, H 6.06, N 4.64, Cl 13.07.

Preparation of [C_4H_4B-NH(CHMe$_2$)$_2$]TaCl$_3$(Me$_2$C(O)CH$_2$C(O)Me) (5). To a solution of **1** (40 mg, 0.089 mmol) in C_6D_6 was added 1 equiv of diacetone alcohol (10.3 mg, 0.0888 mmol) or 2 equiv of spectroscopic grade acetone (10.3 mg, 0.178 mmol). An immediate color change to yellow-orange was observed. X-ray quality crystals were grown from a concentrated pentane solution at −35 °C (yield 41 mg, 97%). ^{1}H NMR (C_6D_6): δ 7.24 (s, 1H, N*H*), 6.46 (m, 2H, C*H*CHB), 5.18 (m, 2H, CHC*H*B), 3.45 (sept, 2H, C*H*Me2), 2.62 (s, 2H, CH_2C(O)Me), 1.69 (s, 3H, CH$_2$C(O)*Me*), 1.06 (s, 6H, (O)CMe_2), 0.92 (d, 6H, CHMe_2), 0.83 (d, 6H, CHMe_2). ^{13}C{^{1}H} NMR (C_6D_6): δ 217.4 (CH$_2$*C*(O)Me), 127.8 (*C*(O)Me$_2$), 120.7 (*C*HCHB), 78.15 (CH*C*HB), 51.2 (*C*HMe2), 49.2 (*C*H$_2$C(O)Me), 33.1 (CH$_2$C(O)*Me*), 29.1 ((O)CMe_2), 20.7 (CHMe_2), 20.2 (CHMe_2). Elemental Analysis: $TaCl_3BNO_2C_{16}H_{29}$, MW = 565.51, Calcd: C 33.95, H 5.13, N 2.48, Cl 18.81. Found: C 33.59, H 5.35, N 2.52, Cl 18.72.

Preparation of [C_4H_4B-N(CHMe$_2$)$_2$]Cp*TaCl$_2$ (6). A 25 mL aliquot of THF (precooled to −35 °C) was added to 63 mg (0.44 mmol) of LiCp* and 200 mg (0.44 mmol) of **1**. The resulting green solution was stirred overnight. Upon removal of THF, the dark green residue was washed with pentane to remove impurities. Recrystallization from 2:1 THF/Et_2O (v/v) afforded 183 mg (75%) of **6** as green microcrystals. ^{11}B NMR (external reference BF$_3$·OEt$_2$): δ 38.9. ^{1}H and ^{13}C NMR spectra and elemental analyses were identical to those previously reported.

Preparation of [C_4H_4B-N(CHMe$_2$)$_2$]Cp*Ta(CO)$_2$ (7). CO(g) (607 Torr) was placed over a frozen, degassed THF solution of [C_4H_4B-N(CHMe$_2$)$_2$]Cp*TaCl$_2$ (101 mg, 0.184 mmol) and excess Mg(s) (109 mg, 4.49 mmol). Upon thawing, the solution color became bright orange. After 1 h at room temperature, the solvent was removed in vacuo, and the product was extracted into pentane. Solvent removal gave 97 mg of the product (98%). X-ray quality crystals were obtained from a concentrated pentane solution at −35 °C. ^{1}H NMR (C_6D_6): δ 4.22 (m, 2H, C*H*CHB), 3.45 (sept, 2H, C*H*Me$_2$), 2.43 (m, 2H, CHC*H*B), 1.64 (s, 15H, C_5Me_5), 1.31 (m, 12H, CHMe_2). ^{13}C{^{1}H} NMR (C_6D_6): δ 227.1 (*C*O), (C_5Me$_5$), 100.6 (*C*HCHB), 83.5 (CH*C*HB), 47.2 (*C*HMe$_2$), 23.0 (CHMe_2), 11.0 (C_5Me_5) FT-IR analysis (in CD_2Cl_2): υ(CO) = 1969, 1893 cm^{-1}. Elemental Analysis: $C_{22}H_{33}BNO_2Ta$, MW = 535.3, Calcd: C 49.39, H 6.17, N 2.62. Found: C 49.92, H 6.11, N 2.76.

Observation of {[C_4H_4B-NH(CHMe$_2$)$_2$]Cp*Ta(CO)$_2$}B(C$_6$H$_3$(CF$_3$)$_2$)$_4$ (8). A solution of 5 mg (0.0093 mmol) of [C_4H_4B-N(CHMe$_2$)$_2$]Cp*Ta(CO)$_2$ in 1 mL of CD_2Cl_2 was prepared and treated with 9 mg (0.0093 mmol) of [H(Et$_2$O)$_2$][B(C$_6$H$_3$(CF$_3$)$_2$)$_4$ dissolved in 1 mL of CD_2Cl_2. The color of the solution changed immediately from orange-yellow to yellow. After stirring this solution for 1 h, the product was used for characterization. All attempts to scale-up and isolate gave oily products. ^{1}H NMR (CD_2Cl_2): δ 7.72 (s, 8H, B(3,5-(CF$_3$)$_2$C$_6$*H*$_3$)$_4$), 7.56 (s, 4H, B(3,5-(CF$_3$)$_2$C$_6$*H*$_3$)$_4$), 4.78 (m, 2H, C*H*CHB), 3.86 (b, 1H, N*H*), 3.62 (sept, 2H, C*H*Me$_2$), 3.42 (q, 4H, *Et*$_2$O), 3.33 (m, CHC*H*B), 2.04 (s, 15H, C_5Me_5), 1.43 (d, 6H, CHMe_2), 1.37 (d, 6H, CHMe_2), 1.15 (t, 6H, *Et*$_2$O). ^{13}C{^{1}H} NMR (CD_2Cl_2): δ 231.8 (*C*O), 162.9 (B(C$_6$H$_3$CF$_3$)$_2$)$_4$, 162.4 (B(C$_6$H$_3$CF$_3$)$_2$)$_4$, 161.9 (B(C$_6$H$_3$(CF$_3$)$_2$)$_4$, 161.4 (B(C$_6$H$_3$(CF$_3$)$_2$)$_4$, 135.2 (C_5Me$_5$), 123.6 (*C*F$_3$), 117.8 (*C*HCHB), 91.1 (CH*C*HB), 55.3 (*C*HMe$_2$), 21.4 (CHMe_2), 21.2 (CHMe_2), 11.5 (C_5Me_5). FT-IR analysis (in CD_2Cl_2): υ(CO) = 2000, 1899 cm^{-1}.

Preparation of [C_5H_4Me][C_4H_4B-N(CHMe$_2$)$_2$]TaCl$_2$ (9). To a stirring THF solution of 52 mg (0.1154 mmol) of **1** was added dropwise 9.9 mg (0.1154 mmol) of [C_5H_4Me]Li dissolved in THF. An instantaneous color change to bright green occurred. After 5 min of stirring at room temperature, the solvent was removed under vacuum. The green product was extracted with pentane to give a yield of 43 mg (76%). ^{1}H NMR (C_6D_6, 298 K): δ 6.56 (m, 2 H, C*H*CHB), 5.98 (m, 2H, C_5H_4Me), 5.66 (m, 2H, C_5H_4Me), 3.38 (sept, 2H, C*H*Me$_2$), 2.65 (m, 2H, CHC*H*B), 2.08 (s, 3H, C_5H_4*Me*), 1.10 (d, 6H, CHMe_2, J = 6.8 Hz), 1.01 (d, 6H, CHMe$_2$, J = 6.7 Hz). ^{13}C{^{1}H} NMR (C_6D_6): δ 131.0 (*C*HCHB), 117.1 (C_5H$_4$Me), 110.2 (C_5H$_4$Me), 47.7 (*C*HMe$_2$), 46.3 (CH*C*HB), 24.5 (C_5H_4*Me*), 23.6 (CHMe_2), 14.2 (CHMe_2).

Preparation of [C_5H_4Me]$_2$[η^2-C_4H_4B-NH(CHMe$_2$)$_2$]TaCl (10). To a THF solution of 40 mg (0.089 mmol) of **1** was added dropwise 27 mg (0.311 mmol) of Li[C_5H_4Me] suspended in THF. An instantaneous color change to green and then orange-yellow was observed. The reaction was stirred at room temperature for 20 min before the solvent was removed in vacuo. The product was obtained by pentane extraction and solvent removal (30 mg, 63%). X-ray quality crystals were obtained from a concentrated pentane solution at −35 °C. ^{1}H NMR (THF-d_8, 298 K): δ 6.94 (d, 1H, C*H*CHB), 5.48 (b, 1H, C_5H_4Me), 5.40 (s, 1H, C_5H_4Me), 5.28 (br, 2H, C_5H_4Me), 5.17 (br, 1H, C*H*CHB), 5.16 (s, 1H, C_5H_4Me), 5.09 (br, 1H, C_5H_4Me), 5.01 (br, 1H, C_5H_4Me), 4.93 (b, 1H, C_5H_4Me), 4.67 (sept, 1H, C*H*Me$_2$), 3.29 (sept, 1H, C*H*Me$_2$), 3.24 (d, 1H, CHC*H*B), 2.07 (s, 3H, C_5H_4*Me*), 2.00 (s, 3H, C_5H_4*Me*), 1.41 (d, 1H, CHC*H*B), 1.23 (d, 12H, CHMe_2). ^{13}C{^{1}H} NMR (THF-d_8): δ 132.8 (*C*HCHB), 108.2 (C_5H$_4$Me), 108.7 (C_5H$_4$Me), 101.8 (C_5H$_4$Me), 99.8 (*C*HCHB), 96.8 (C_5H$_4$Me), 96.3 (C_5H$_4$Me), 64.0 (C_5H$_4$Me), 52.3 (C_5H$_4$Me), 48.9 (*C*HMe$_2$), 45.2 (*C*HMe$_2$), 44.4 (CH*C*HB), 26.9 (C_5H_4*Me*), 26.6 (C_5H_4*Me*), 23.9 (CH*C*HB), 16.2 (CHMe_2), 14.8 (CHMe_2). ^{11}B NMR (external reference BF$_3$·OEt$_2$): δ 49.2. Elemental Analysis: $C_{22}H_{32}BClNTa$ MW = 537.7, Calcd: C 49.10, H 5.95, N 2.60, Cl 6.59. Found: C 49.42, H 5.80, N 2.81, Cl 6.81.

Preparation of [C_4H_4B-N(CHMe$_2$)$_2$]Ta[C_5H_5B-C_6H_5]Cl$_2$ (11). A solution of 100 mg (0.644 mmol) of Li[C_5H_5B-C_6H_5] in 40 mL of Et_2O was slowly added to a solution containing 145 mg (0.322 mmol) of **1** in 5 mL of Et_2O. The resulting green solution was allowed to stir at room temperature for 10 min before removing the solvent in vacuo. The product was extracted with pentane, and the resulting solution filtered. X-ray quality crystals were grown from a concentrated pentane solution at −35 °C in 82% yield. ^{1}H NMR (C_6D_6): δ 7.86 (d, 2H, *o*-C$_6$*H*$_5$), 7.30 (m, 3H, C$_6$*H*$_5$), 6.68 (dd, 2H, CHC*H*CHB), 6.05 (t, 1H, C*H*CHCHB), 5.94 (d, 2H, CHCHC*H*B), 5.60 (m, 2H, C*H*CHB), 3.84 (m, 2H, CHC*H*B) 3.64 (sept, 2H, C*H*Me$_2$), 1.15 (d, 6H, CHMe_2), 1.01 (d, 6H, CHMe_2). ^{13}C{^{1}H} NMR (C_6D_6): δ 144.5 (C_6H$_5$), 137.2 (C_6H$_5$), 133.7 (C_6H$_5$), 131.2 (CH*C*HCHB), 128.7 (C_6H$_5$), 123.5 (CHCH*C*HB), 110.0 (*C*HCHCHB), 105.9 (*C*HCHB), 93.5 (CH*C*HB), 47.2 (*C*HMe$_2$),

25.0 (CH*Me*$_2$), 24.0 (CH*Me*$_2$). ^{11}B NMR (external reference BF_3·OEt_2): δ 38.5 (C_4H_4*B*N(CHMe$_2$)$_2$), 35.0 (C_5H_5*B*Ph). Elemental Analysis: $C_{21}H_{28}B_2Cl_2Ta$, M = 567.9, Calcd: C 44.41, H 4.93, N 2.47, Cl 12.48. Found: C 44.01, H 5.22, N 2.31, Cl 12.21.

Preparation of [C_4H_4B-N(CHMe$_2$)$_2$]Ta[C_5H_5B-NMe$_2$]Cl$_2$ (12). To a stirring solution of **1** (100 mg, 0.222 mmol) in 10 mL of Et_2O was added dropwise Li[C_5H_5B-NMe$_2$] (28.2 mg, 0.222 mmol) dissolved in 5 mL of Et_2O. The solution became a pea-green color upon completion of the addition. Removal of solvent under vacuum gave the product as a red solid (100 mg, 84%). X-ray quality crystals were obtained from a concentrated Et_2O solution at −35 °C. ^{1}H NMR (C_6D_6): δ 6.39 (m, 2H, CHC*H*CHB), 5.82 (m, 2H, C*H*CHB), 5.72 (t, 1H, C*H*CHCHB), 4.81 (d, 2H, CHCHC*H*B), 3.93 (m, 2H, CHC*H*B), 3.76 (sept, 2H, C*H*Me$_2$), 2.46 (s, 6H, N*Me*$_2$), 1.29 (d, 6H, CH*Me*$_2$), 1.09 (d, 6H, CH*Me*$_2$); ^{13}C{^{1}H} NMR (C_6D_6): δ 142.4 (CH*C*HCHB), 127.8 (CHCHB), 122.9 (*C*HCHCHB), 97.8 (CHCH*C*HB), 92.0 (CH*C*HB), 46.7 (*C*HMe$_2$), 37.6 (N*Me*$_2$), 24.2 (CH*Me*$_2$), 23.9 (CH*Me*$_2$). ^{11}B NMR (external reference BF_3·OEt_2): δ 38.2 (C_4H_4*B*N(CHMe$_2$)$_2$), 26.8 (C_5H_5*B*NMe$_2$). Elemental Analysis: $C_{17}H_{29}B_2N_2Cl_2Ta$, M = 534.9, Calcd: C 38.17, H 5.43, N 5.24, Cl 13.25. Found: C 38.12, H 5.58, N 5.16, Cl 12.04.

Preparation of [C_4H_4B-N(CHMe$_2$)$_2$]Ta[C_5H_5B-N(CHMe$_2$)$_2$]Cl$_2$ (13). A precooled (−35 °C) solution of lithium diisopropylamide, freshly prepared from 57.5 mg (56.4 mmol) of diisopropylamine and 0.35 mL of *n*-BuLi (1.6 M in hexanes) in approximately 10 mL of Et_2O, was added dropwise to a stirred solution of 100 mg (56.4 mmol) [C_5H_6B-N(CHMe$_2$)$_2$] in 5 mL of Et_2O (also precooled to −35 °C). The resulting solution was allowed to stir for 45 min. After cooling to −35 °C, the solution was slowly added to a cold (−35 °C) solution containing 254 mg (56.4 mmol) of **1** in 10 mL of Et_2O. The resulting dark green solution was stirred for 1 h. After removal of all volatiles, the residue was extracted with pentane. The extract was filtered, and the pentane removed to give a dark green oil. The product was recrystallized from Et_2O by slow evaporation at −35 °C (122 mg, 37%). ^{1}H NMR (C_6D_6): δ 6.40 (m, 2H, CHC*H*CHB), 5.98 (m, 2H, C*H*CHB), 5.65 (t, 1H, J = 6.6 Hz, C*H*CHCHB), 4.99 (m, 2H, CHCHC*H*B), 3.97 (m, 2H, CHC*H*B), 3.75 (sept, 2H, C_4H_4BNC*H*), 3.41 (br, 2H, C_5H_5-BNC*H*), 1.29 (d, 6H, J = 6.8 Hz, C_4H_4BNCH*Me*$_2$), 1.10 (d, 6H, J = 6.8 Hz, C_4H_4BNCH*Me*$_2$), 1.03 (d, 12H, J = 6.9 Hz, C_5H_5BNCH*Me*$_2$). ^{13}C{^{1}H} NMR (C_6D_6): δ 141.6 (CH*C*HCHB), 123.4 (*C*HCHB), 102.0 (CHCH*C*HB), 97.3 (*C*HCHCHB), 91.2 (CH*C*HB), 46.7 (C_4H_4BN*C*H), 46.3 (C_5H_5BN*C*H), 24.1 (C_4H_4BNCH*Me*$_2$), 24.0 (C_5H_5BNCH*Me*$_2$), 23.2 (C_4H_4BNCH*Me*$_2$), 22.8 (C_5H_5BNCH*Me*$_2$). Elemental Analysis: $C_{21}H_{37}B_2Cl_2N_2Ta$, MW = 591.0, Calcd: C 42.68, H 6.31, N 4.74. Found: C 42.81, H 6.41, N 4.72.

Preparation of [C_4H_4B-NH(CHMe$_2$)$_2$]TaCl$_4$ (1·HCl). A solution of **1** in C_6D_6 (approximately 10 mg in 750 μL) was placed inside an NMR tube, and 1 mL of dry HCl was syringed through a rubber septum. Quantitative formation of **1·HCl** was observed. Crystalline samples can be obtained by cooling a concentrated toluene solution. ^{1}H NMR (C_6D_6): δ 6.35 (m, 2H, C*H*CHB), 6.18 (br, 1H, N*H*), 4.98 (m, 2H, CHC*H*B), 3.09 (sept., 2H, C*H*Me$_2$), 0.64 (d, 6H, CH*Me*$_2$), 0.58 (d, 6H, CH*Me*$_2$). ^{13}C{^{1}H} NMR (C_6D_6): δ 122.7 (*C*HCHB), 109.9 (br, CH*C*HB), 52.3 (*C*HMe$_2$), 20.5 (CH*Me*$_2$), 19.9 (CH*Me*$_2$). ^{11}B (external reference BF_3·OEt_2): δ 30.8. Elemental Analysis: $C_{10}H_{19}BCl_4NTa$ MW = 486.8, Calcd: C 24.65, H 3.90, N 2.88. Found: C 25.90, H 3.49, N 2.71.

Preparation of [C_4H_4B-N(CHMe$_2$)$_2$]Ta[C_5H_5B-C_6H_5]Me$_2$ (14). To a stirring solution of [C_4H_4B-N(CHMe$_2$)$_2$]Ta[C_5H_5B-C_6H_5]Cl$_2$ (160 mg, 0.322 mmol) in 10 mL of Et_2O was added dropwise a suspended solution of methyllithium (14.2 mg, 0.644 mmol) in 5 mL of Et_2O. The solution instantly turned blue. After stirring for 20 min, the solvent was removed in vacuo, and the product was extracted with pentane. The extract was filtered, and the pentane was removed to give a blue oil which is difficult to crystallize. Solids were obtained by slowly cooling a concentrated pentane solution. ^{1}H NMR (C_6D_6): δ 7.80 (d, 2H, *o*-C_6H_5), 7.33 (m, 2H, *m*-C_6H_5), 7.28 (t, 1H, *p*-C_6H_5), 6.55 (dd, 2H, CHC*H*CHB), 6.01 (t, 1H, C*H*CHCHB), 5.62 (d, 2H, CHCHC*H*B), 5.50 (m, 2H, C*H*CHB), 3.74 (m, 2H, CHC*H*B), 3.54 (sept, 2H, C*H*Me$_2$), 1.07 (d, 6H, CH*Me*$_2$), 1.02 (d, 6H, CH*Me*$_2$), 0.29 (s, 6H, Ta*Me*$_2$). ^{13}C-{^{1}H} NMR (C_6D_6): δ 137.5 (C_6H_5), 133.2 (C_6H_5), 130.0 (C_6H_5), 129.1 (C_6H_5), 128.3 (CH*C*HCHB), 128.2 (*C*HCHCHB), 111.3 (CHCH*C*HB), 105.9 (*C*HCHB), 91.2 (CH*C*HB), 47.2 (*C*HMe$_2$), 29.3 (CH*Me*$_2$), 27.6 (CH*Me*$_2$), 22.8 (Ta*Me*$_2$). ^{11}B NMR (external reference BF_3·OEt_2): δ 36.5 (C_4H_4*B*N(CHMe$_2$)$_2$), 35.0 (C_5H_5*B*C_6H_5). Elemental Analysis: $C_{23}H_{34}B_2NTa$, MW = 527.0, Calcd: C 52.37, H 6.45, N 2.66. Found: C 52.71, H 6.23, N 2.55.

Preparation of [C_4H_4B-N(CHMe$_2$)$_2$]Ta[C_5H_5B-NMe$_2$]Me$_2$ (15). To a stirring solution of [C_4H_4B-N(CHMe$_2$)$_2$]Ta[C_5H_5B-NMe$_2$]Cl$_2$ (20 mg, 0.037 mmol) in 10 mL of Et_2O was added dropwise methyllithium (53 μL, 0.074 mmol, 1.4 M in Et_2O). The resulting blue solution was stirred for 10 min before removing solvent. The product was then extracted with pentane and filtered. The product was recrystallized from pentane by slow evaporation at −35 °C (15 mg, 82%). ^{1}H NMR (C_6D_6): δ 6.20 (dd, 2H, CHC*H*CHB), 5.82 (t, 1H, C*H*CHCHB), 5.78 (m, 2H, C*H*CHB), 4.57 (d, 2H, CHCHC*H*B), 3.84 (m, 2H, CHC*H*B), 3.66 (sept. 2H, C*H*Me$_2$), 2.50 (s, 6H, N*Me*$_2$), 1.20 (d, 6H, CH*Me*$_2$), 1.08 (d, 6H, CH*Me*$_2$), 0.13 (s, 6H, Ta*Me*$_2$). ^{13}C{^{1}H} NMR (C_6D_6): δ 136.2 (CH*C*HCHB), 111.6 (*C*HCHCHB), 99.5 (*C*HCHB), 97.9 (CHCH-*C*HB), 88.6 (CH*C*HB), 47.2 (*C*HMe$_2$), 39.6 (N*Me*$_2$), 23.0 (CH*Me*$_2$), 22.4 (CH*Me*$_2$), 21.2 (Ta*Me*$_2$). Elemental Analysis: $C_{19}H_{35}B_2N_2Ta$, MW = 493.6, Calcd: C 46.19, H 7.09, N 5.67. Found: C 45.80, H 7.05, N 5.41.

Preparation of [C_4H_4B-N(CHMe$_2$)$_2$]Ta[C_5H_5B-C_6H_5](PMe$_3$)$_2$ (16). To a resealable NMR tube containing [C_4H_4B-N(CHMe$_2$)$_2$]Ta[C_5H_5B-C_6H_5]Me$_2$ (31 mg, 0.0546 mmol) in C_6D_6 was added 18 mL (0.109 mmol) of PMe_3. The tube was then degassed, and 620 Torr H_2 was placed over the frozen sample. After 1 h of rotation (to allow for hydrogen diffusion into the solution), the orange product appears. The product was isolated after removal of solvent and Et_2O extraction (19 mg, 54%). X-ray quality crystals were grown from a concentrated Et_2O solution vapor diffused with pentane. ^{1}H NMR (C_6D_6): δ 7.98 (d, 2H, *o*-C_6H_5), 7.32 (m, 2H, *m*-C_6H_5), 7.14 (t, 1H, *p*-C_6H_5), 5.08 (m, 2H, CHC*H*CHB), 4.62 (t, 1H, C*H*CHCHB), 4.16 (b, 2H, CHCHC*H*B), 3.97 (m, 2H, C*H*CHB), 3.49 (sept, 2H, C*H*Me$_2$), 2.10 (b, 2H, CHC*H*B), 1.42 (d, 6H, CH*Me*$_2$), 1.19 (d, 6H, CH*Me*$_2$), 0.90 (d, 18H, P*Me*$_3$). ^{13}C-{^{1}H} NMR (C_6D_6): δ 136.1 (C_6H_5), 134.3 (C_6H_5), 131.6 (C_6H_5), 97.7 (CHC*H*CHB), 96.87 (*C*HCHCHB), 83.5 CHCH*C*HB), 80.0 (*C*HCHB), 46.8 (*C*HMe$_2$), 34.38 (CH*C*HB), 24.2 (CH*Me*$_2$), 22.8 (CH*Me*$_2$), 22.5 (P*Me*$_3$). Elemental Analysis: $C_{27}H_{46}B_2NP_2Ta$, MW = 649.2, Calcd: C 49.96, H 7.09, N 2.16. Found: C, 46.54, H, 7.19, N, 1.92.

Preparation of [C_4H_4B-N(CHMe$_2$)$_2$]Ta[C_5H_5B-C_6H_5](H)$_2$(PEt$_3$) (17). To a solution of [C_4H_4B-N(CHMe$_2$)$_2$]Ta[C_5H_5B-C_6H_5]Me$_2$ (17 mg, 0.0372 mmol) in C_6D_6 was added 2 equiv of PEt_3 (11 μL, 0.74 mmol) via microliter syringe. The sample was degassed using three freeze−pump−thaw cycles, and 434 Torr of H_2 was placed over the frozen sample. The solution was thawed and allowed to rotate for 5 days. The solvent was removed in vacuo, and the product was extracted with Et_2O and filtered. Crystals suitable for X-ray analysis were grown from a concentrated Et_2O solution at −35 °C. ^{1}H NMR (C_6D_6): δ 8.01 (d, 2H, *o*-C_6H_5), 7.44 (m, 2H, *m*-C_6H_5), 7.29 (t, 1H, *p*-C_6H_5), 6.23 (m, 2H, CHC*H*CHB), 5.02 (t, 1H, C*H*CHCHB), 4.91 (m, 2H, C*H*CHB), 4.26 (d, 2H, CHCHC*H*B), 3.33 (sept, 2H, C*H*Me$_2$), 2.55 (m, 2H, CHC*H*B), 1.24 (d, 12H, CH*Me*$_2$), 0.99 (m, 6H, PCH_2CH$_3$), 0.53 (m, 9H, PCH$_2$C*H*$_3$), −2.58 (d, 2H, TaH_2, J_{PH} = 59.5 Hz). ^{13}C{^{1}H} NMR (C_6D_6): δ 133.8 (C_6H_5), 129.0 (C_6H_5), 128.2 (C_6H_5), 127.2 (C_6H_5), 121.0 (CH*C*HCHB), 95.5 (*C*HCHCHB), 87.3 (*C*HCHB), 76.5 (CH*C*HB), 58.5 (CHCH*C*HB), 47.0 (*C*HMe$_2$), 22.9 (CH*Me*$_2$), 21.1 (PCH_2CH$_3$), 7.7 (PCH$_2$*C*H$_3$). ^{31}P{^{1}H} NMR (C_6D_6): δ 10.1 (Ta(*P*CH$_2$CH$_3$)$_3$). ^{11}B NMR (external reference BF_3·OEt_2): δ 33.7 (C_4H_4*B*N(CHMe$_2$)$_2$), 19.4 (C_5H_5*B*C_6H_5). Elemental Analysis: $C_{27}H_{45}B_2NPTa$, MW = 617.2, Calcd: C 52.55, H 7.29, N 2.27. Found: C 52.44, H 7.57, N 2.49.

Preparation of {[C_4H_4B-N(CHMe$_2$)$_2$]Ta(PMe$_3$)$_2$ClN}$_2$ (18). THF and PMe_3 (122 mg, 1.62 mmol) were vacuum transferred onto dry **1** (145 mg, 0.322 mmol) and Mg (39 mg, 1.63 mmol) at −78 °C. This solution was allowed to warm to room temperature and stirred for 2 h. Solvent was removed in vacuo, and the solid orange product was isolated in a nitrogen containing glovebox by washing with benzene (yield 125 mg, 35%). X-ray quality crystals were grown from a dilute pentane solution. ^{1}H NMR (C_6D_6): δ 5.13 (m, 2H, C*H*CHB), 3.65 (sept, 2H, C*H*Me$_2$), 3.36 (m, 2H, CHC*H*B), 1.35 (t, 18H, (P*Me*$_3$)$_2$), 1.30 (d, 12H, CH*Me*$_2$). ^{13}C{^{1}H} NMR (C_6D_6): δ 100.5 (*C*HCHB),

Table 3. Crystal and Structure Refinement Data for **1**, **3**, **4**, and **5**

	1	**3**	**4**	**5**
chemical formula	$C_{10}H_{18}BCl_3NTa$	$C_{17}H_{37}BCl_2NSi_2Ta$	$C_{22}H_{36}BCl_2NTa$	$C_{16}H_{29}BCl_3NO_2Ta$
formula weight	450.38	574.32	587.15	565.51
crystal system	monoclinic	triclinic	monoclinic	monoclinic
space group (no.)	$P2_1/c$ (#14)	$P\bar{1}$ (#2)	$P2_1/n$ (#14)	$C2/c$ (#15)
color of crystal	purple	dark green	orange	yellow
Z	4	2	4	8
a, Å[a]	17.078(3)	6.753(2)	16.531(3)	30.4978(2)
b, Å	7.859(2)	8.403(2)	9.599(2)	10.7693(2)
c, Å	11.070(2)	21.917(4)	17.259(4)	14.3058(2)
α, deg	90.00	84.33(3)	90.00	90.00
β, deg	97.81(3)	86.07(3)	114.64(3)	114.419(1)
γ, deg	90.00	75.82(3)	90.00	90.00
volume, Å^3	1471.9(5)	1198.6(4)	2489.4(9)	4278.29(10)
temp, K	213(2)	213(2)	223(2)	193(2)
total no. reflcns	2951	4580	10014	11965
no. of obsd data[c]	2587	4185	3204	4821
no. of params varied	146	217	247	217
$R_1(F_o)$, $wR_2(F_o^2)$ %[b,c]	4.45, 10.67	4.40, 12.11	4.48, 9.33	2.88, 5.21
goodness-of-fit on F^2	1.041	1.031	1.272	1.071

Table 4. Crystal and Structure Refinement Data for **7**, **10**, **11**, and **12**

	7	**10**	**11**	**12**
chemical formula	$C_{22}H_{33}BNO_2Ta$	$C_{22}H_{32}BClNTa$	$C_{21}H_{28}B_2Cl_2NTa$	$C_{17}H_{29}B_2Cl_2N_2Ta$
formula weight	535.25	537.70	567.91	534.89
crystal system	monoclinic	monoclinic	monoclinic	monoclinic
space group (no.)	$P2_1/c$ (#14)	$P2_1/n$ (#14)	$P2_1/c$ (#14)	$P2_1/n$ (#14)
color of crystal	orange	orange	green	orange
Z	4	4	8	4
a, Å[a]	14.185(3)	7.8620(11)	10.402(1)	9.7287(4)
b, Å	13.936(3)	20.291(2)	19.4450(3)	18.8762(8)
c, Å	11.408(2)	13.702(2)	22.2663(1)	11.6704(5)
β, deg	93.57(3)	105.21(9)	100.725(1)	97.73(1)
volume, Å^3	2250.8(8)	2109.2(4)	4425.10(7)	2123.7(2)
temp, K	243(2)	193(2)	223(2)	223(2)
total no. reflcns	3967	13055	26358	12976
no. of obsd data[c]	3948	4991	8288	2747
no. of params varied	245	235	488	177
$R_1(F_o)$, $wR_2(F_o^2)$ %[b,c]	5.20, 8.92	2.13, 4.91	4.26, 12.95	5.76,10.94
goodness-of-fit on F^2	0.999	1.071	1.028	1.200

Table 5. Crystal and Structure Refinement Data for **16**−**19**

	16	**17**	**18**	**19**
chemical formula	$C_{27}H_{46}B_2NP_2Ta$	$C_{27}H_{45}B_2NPTa$	$C_{32}H_{72}B_2Cl_2N_4P_4Ta_2$	$C_{19}H_{45}BClNP_3Ta$
formula weight	649.16	617.18	1090.90	607.68
crystal system	orthorhombic	monoclinic	monoclinic	monoclinic
space group (no.)	*Pbca* (#61)	$P2_1/c$ (#14)	$P2_1/c$ (#14)	$P2_1/c$ (#14)
color of crystal	red-orange	yellow	orange	red
Z	8	4	4	8
a, Å[a]	12.1379(2)	21.2399 (3)	11.308(1)	9.252(2)
b, Å	18.637(1)	8.2213(2)	33.275(4)	19.144(3)
c, Å	25.0371(3)	15.9203(2)	13.198(1)	30.2930(1)
β, deg	90.000(1)	100.293(9)	98.348(9)	90.870(2)
volume, Å^3	5663.59(12)	2735.26(8)	4913.4(9)	5365.30(14)
temp, K	193(2)	193(2)	193(2)	193(2)
total no. reflcns	19792	15545	19204	34195
no. of obsd data[c]	3677	5001	6349	12979
no. of params varied	298	297	424	469
$R_1(F_o)$, wR_2 (F_o^2) %[b,c]	4.94, 7.06	3.21, 5.50	4.05, 7.41	4.75, 7.10
goodness-of-fit on F^2	1.215	1.014	1.123	1.127

77.0 (CHCHB), 48.1 (*C*HMe$_2$), 23.6 (CH*Me$_2$*), 14.6 (P*Me$_3$*). FT-IR analysis (in THF): υ(NN) = 1720 cm^{-1}. Elemental Analysis: $C_{32}H_{72}B_2Cl_2N_4P_4Ta_2$, MW = 1090.9, Calcd: C 35.20, H 6.60, N 5.13. Found: C 35.95, H 6.69, N 5.03.

Preparation of [C$_4$H$_4$B-N(CHMe$_2$)$_2$]Ta(PMe$_3$)$_3$Cl (19). Degassed THF and PMe$_3$ (123.2 mg, 1.62 mmol) were vacuum transferred onto **1** (146 mg, 0.324 mmol) and Mg (39 mg, 1.62 mmol) at −78 °C. This solution was allowed to warm to room temperature and stirred for 2 h. Solvent was removed in vacuo, and the cherry red product was extracted into pentane and filtered. This solution was brought into an argon atmosphere box, and X-ray quality crystals were grown from a concentrated pentane solution (yield 125 mg, 63%). ^{1}H NMR (C_6D_6): δ 3.82 (m, 2H, C*H*CHB), 3.70 (sept, 2H, C*H*Me$_2$), 2.80 (m, 2H, CHC*H*B), 1.43 (d, 12H, CH*Me$_2$*), 1.23 (br, 27H, (PMe$_3$)$_3$). ^{13}C{^{1}H} NMR (C_6D_6): δ 78.8 (*C*HCHB), 68.4 (CH*C*HB), 47.8 (*C*HMe$_2$), 24.8 (CH*Me$_2$*), 14.5 (P*Me$_3$*). Elemental Analysis: $C_{19}H_{45}BClNP_3Ta$, MW = 607.7, Calcd C 37.53, H 7.41, N 2.30. Found: C 37.82, H 7.27, N 2.45.

Table 6. Crystal and Structure Refinement Data for **20**

	20
chemical formula	$C_{29}H_{65}B_2Cl_2N_2P_3Ta_2$
formula weight	989.30
crystal system	triclinic
space group (no.)	$P\bar{1}$ (#2)
color of crystal	red
Z	4
a, Å[a]	11.9386(1)
b, Å	17.5654(3)
c, Å	21.8901(3)
α, deg	89.737(1)
β, deg	87.384(1)
γ, deg	83.75(1)
volume, Å^3	4558.5 (1)
temp, K	213(2)
total no. reflcns	27474
no. of obsd data[c]	19298
no. of params varied	819
$R_1(F_o)$, $wR_2(F_o^2)$ %[b,c]	3.99, 8.72
goodness-of-fit on F^2	1.084

[a] It has been noted that the integration program SAINT produces cell constant errors that are unreasonably small, since systematic error is not included. More reasonable errors might be estimated at 10× the listed values. [b] $R_1 = (\sum||F_o| - |F_c||)/\sum|F_o|$, $wR_2 = [\sum[w(F_o^2 - F_c^2)^2]/\sum[w(F_o^2)^2]]^{1/2}$, where $w = 1/[\sigma^2(F_o^2) + (a\cdot P)^2 + b\cdot P]$ and $P = [f\cdot(\text{maximum of 0 or } F_o^2) + (1-f)\cdot F_c^2]$. [c] ($I > 2\sigma(I)$).

Preparation of ([C_4H_4B-N(CHMe$_2$)$_2$]Ta(H)(PMe$_3$)Cl)μ-H([C_4H_4BN-(CHMe$_2$)$_2$]Ta(PMe$_3$)$_2$Cl) (20). To a degassed, frozen benzene solution of **19** (30 mg, 0.049 mmol) was added excess hydrogen gas. The solution was thawed and allowed to stir at room temperature for 5 days. The red product was washed with cold pentane, then taken up in pentane, and filtered. X-ray quality crystals were grown from a concentrated pentane solution at −35 °C over 2 days (40 mg, 82%). ^{1}H NMR (THF-d_8): δ 7.61 (m, 1H, Ta-*H*-Ta, J_{PH} = 72.9 Hz), 5.79 (s, 1H, C*H*CHB, ring 1), 5.13 (s, 1H, C*H*CHB, ring 2), 5.12 (s, 1H, C*H*CHB, ring 2), 4.58 (s, 1H, C*H*CHB, ring 1), 3.22 (sept, 2H, C*H*Me$_2$), 2.89 (s, 1H, CHC*H*B, ring 2), 2.61 (s, 1H, CHC*H*B, ring 1), 2.41 (s, 1H, CHC*H*B, ring 2), 2.15 (m, 1H, CHC*H*B, ring 1), 1.93 (br d, 9H, PMe$_3$), 1.68 (d, 9H, PMe$_3$ coupled to terminal hydride), 1.46 (d, 9H, PMe$_3$, coupled to bridging hydride), 1.19 (d, 6H, CHMe$_2$), 1.12 (d, 6H, CHMe$_2$), −2.78 (m, 1H, Ta−H, J_{PH} = 28.2 Hz). ^{31}P{^{1}H} NMR (C_6D_6): δ -5.1 (d, J_{PP} = 53.1 Hz), −6.6 (d, J_{PP} = 7.1 Hz), −10.6 (dd, J_{PP} = 53.2 Hz, J_{PP} = 6.9 Hz). ^{11}B{^{1}H} NMR (C_6D_6): δ 28.2 (br, CHCH*B*), 14.6 (br, CHCHCH*B*). ^{13}C{^{1}H} NMR (C_6D_6): δ 100.5 (*C*HCHB), 94.3 (*C*HCHB), 93.7 (*C*HCHB), 91.2 (*C*HCHB), 81.0 (CH*C*HB), 72.8 (CH*C*HB), 71.8 (CH*C*HB), 67.9 (CH*C*HB), 47.7 (*C*HMe$_2$), 24.1 (CH*Me$_2$*), 23.9 (CH*Me$_2$*), 17.7 (P*Me$_3$*, J_{PC} = 11.9 Hz), 17.4 (P*Me$_3$*, J_{PC} = 11.6 Hz), 16.4 (P*Me$_3$*). Elemental Analysis: $C_{29}H_{65}B_2Cl_2N_2P_3Ta_2$, MW = 989.3 Calcd: (with one pentane molecule) C 38.47, H 7.33, N 2.64, Cl 6.68. Found: C 38.33, H 7.40, N 3.52, Cl 6.56.

Structure Determinations. Crystals of **1**, **3**, and **7** were mounted under a flow of nitrogen onto a glass fiber with epoxy. These were then placed on the diffractometer (Enraf-Nonius-CAD4) in a cold nitrogen stream. An empirical absorption correction using the program DIFABS[55] was applied to **3**. The structure of **3** was determined by heavy-atom Patterson methods (DIRDIF−Patty: teXsan)[56] and refined by SHELXTL 5.04.

Crystals of **4**, **5**, **10**, **11**, **12**, **16**, **17**, **18**, **19**, and **20** were mounted on glass fibers under Paratone-8277 and placed on the X-ray diffractometer in a cold nitrogen stream supplied by a Siemens LT-2A low-temperature device. The X-ray intensity data were collected on a standard Siemens SMART-CCD Area Detector System equipped with a normal focus molybdenum-target X-ray tube operated at 1.5 kW (50 kV, 30 mA) for **4**, **11**, and **12** and at 2.0 kW (50 kV, 40 mA) for **5**, **10**, **16**, **17**, **18**, **19**, and **20**. A total of 1.3 hemispheres of data were collected using a narrow frame method with scan widths of 0.3° in ω and exposure times ranging from 5 to 30 s/frame. Frames were integrated to 0.75 with the Siemens SAINT program. The space groups were assigned on the basis of systematic absences and intensity statistics by using the XPREP program.[57] The structures were solved by direct methods and refined by full-matrix least-squares on F^2. Data for all structures were corrected for absorption either by using SADABS or the correction program in XPREP. Non-hydrogen atoms were refined with anisotropic thermal parameters except for those involving disorder problems as discussed in the text. H atoms were included in idealized positions for all structures except **17** and **20** in which the tantalum hydrides and bridging hydrides, respectively, were located and refined, and the remaining hydrogens were included in idealized positions. Data collection and refinement parameters for the structures are given in Tables 3−6.

Acknowledgment. G.C.B. is an Alfred Sloan Fellow and an Henry and Camille Dreyfus Teacher Scholar. The authors are grateful to these agencies and to the Petroleum Research Fund (ACS) for financial assistance.

Supporting Information Available: Complete crystallographic information (142 pages, print/PDF). See any current masthead page for ordering information and Web access instructions.

JA9741887

(55) *DIFABS*: Walker, N.; Stuart, *Acta Crystallogr.* **1983**, *A39*, 158−166. An empirical absorption correction program.

(56) *TEXSAN*: *Single-Crystal Structure Analysis Software*; Molecular Structure Corporation: The Woodlands, TX, 1993.

(57) *SHELXTL*: *Structure Analysis Program 5.04*; Siemens Industrial Automation, Inc.: Madison, WI, 1995.